Westinghouse Electric Corporation
Energy Systems

Box 355
Pittsburgh Pennsylvania 15230-0355

AW-95-901

November 10, 1995

Document Control Desk
U.S. Nuclear Regulatory Commission
Washington, D.C. 20555

ATTENTION: MR. T. R. QUAY

APPLICATION FOR WITHHOLDING PROPRIETARY INFORMATION FROM PUBLIC DISCLOSURE

SUBJECT: WESTINGHOUSE RESPONSES TO NRC REQUESTS FOR ADDITIONAL INFORMATION ON THE AP600

Dear Mr. Quay:

The application for withholding is submitted by Westinghouse Electric Corporation ("Westinghouse") pursuant to the provisions of paragraph (b)(1) of Section 2.790 of the Commission's regulations. It contains commercial strategic information proprietary to Westinghouse and customarily held in confidence.

The proprietary material for which withholding is being requested is identified in the proprietary version of the subject report. In conformance with 10CFR Section 2.790, Affidavit AW-95-901 accompanies this application for withholding setting forth the basis on which the identified proprietary information may be withheld from public disclosure.

Accordingly, it is respectfully requested that the subject information which is proprietary to Westinghouse be withheld from public disclosure in accordance with 10CFR Section 2.790 of the Commission's regulations.

Correspondence with respect to this application for withholding or the accompanying affidavit should reference AW-95-901 and should be addressed to the undersigned.

Very truly yours,

Brian A. McIntyre, Manager
Advanced Plant Safety and Licensing

/nja

cc: Kevin Bohrer NRC 12H5

2619A

AFFIDAVIT

COMMONWEALTH OF PENNSYLVANIA:

ss

COUNTY OF ALLEGHENY:

Before me, the undersigned authority, personally appeared Brian A. McIntyre, who, being by me duly sworn according to law, deposes and says that he is authorized to execute this Affidavit on behalf of Westinghouse Electric Corporation ("Westinghouse") and that the averments of fact set forth in this Affidavit are true and correct to the best of his knowledge, information, and belief:

Brian A. McIntyre, Manager
Advanced Plant Safety and Licensing

Sworn to and subscribed
before me this 10 day
of November, 1995

Notary Public

Notarial Seal
Rose Marie Payne, Notary Public
Monroeville Boro, Allegheny County
My Commission Expires Nov. 4, 1996
Member, Pennsylvania Association of Notaries

(1) I am Manager, Advanced Plant Safety And Licensing, in the Advanced Technology Business Area, of the Westinghouse Electric Corporation and as such, I have been specifically delegated the function of reviewing the proprietary information sought to be withheld from public disclosure in connection with nuclear power plant licensing and rulemaking proceedings, and am authorized to apply for its withholding on behalf of the Westinghouse Energy Systems Business Unit.

(2) I am making this Affidavit in conformance with the provisions of 10CFR Section 2.790 of the Commission's regulations and in conjunction with the Westinghouse application for withholding accompanying this Affidavit.

(3) I have personal knowledge of the criteria and procedures utilized by the Westinghouse Energy Systems Business Unit in designating information as a trade secret, privileged or as confidential commercial or financial information.

(4) Pursuant to the provisions of paragraph (b)(4) of Section 2.790 of the Commission's regulations, the following is furnished for consideration by the Commission in determining whether the information sought to be withheld from public disclosure should be withheld.

(i) The information sought to be withheld from public disclosure is owned and has been held in confidence by Westinghouse.

(ii) The information is of a type customarily held in confidence by Westinghouse and not customarily disclosed to the public. Westinghouse has a rational basis for determining the types of information customarily held in confidence by it and, in that connection, utilizes a system to determine when and whether to hold certain types of information in confidence. The application of that system and the substance of that system constitutes Westinghouse policy and provides the rational basis required.

Under that system, information is held in confidence if it falls in one or more of several types, the release of which might result in the loss of an existing or potential competitive advantage, as follows:

(a) The information reveals the distinguishing aspects of a process (or component, structure, tool, method, etc.) where prevention of its use by any of Westinghouse's competitors without license from Westinghouse constitutes a competitive economic advantage over other companies.

(b) It consists of supporting data, including test data, relative to a process (or component, structure, tool, method, etc.), the application of which data secures a competitive economic advantage, e.g., by optimization or improved marketability.

(c) Its use by a competitor would reduce his expenditure of resources or improve his competitive position in the design, manufacture, shipment, installation, assurance of quality, or licensing a similar product.

(d) It reveals cost or price information, production capacities, budget levels, or commercial strategies of Westinghouse, its customers or suppliers.

(e) It reveals aspects of past, present, or future Westinghouse or customer funded development plans and programs of potential commercial value to Westinghouse.

(f) It contains patentable ideas, for which patent protection may be desirable.

There are sound policy reasons behind the Westinghouse system which include the following:

(a) The use of such information by Westinghouse gives Westinghouse a competitive advantage over its competitors. It is, therefore, withheld from disclosure to protect the Westinghouse competitive position.

(b) It is information which is marketable in many ways. The extent to which such information is available to competitors diminishes the Westinghouse ability to sell products and services involving the use of the information.

(c) Use by our competitor would put Westinghouse at a competitive disadvantage by reducing his expenditure of resources at our expense.

(d) Each component of proprietary information pertinent to a particular competitive advantage is potentially as valuable as the total competitive advantage. If competitors acquire components of proprietary information, any one component may be the key to the entire puzzle, thereby depriving Westinghouse of a competitive advantage.

(e) Unrestricted disclosure would jeopardize the position of prominence of Westinghouse in the world market, and thereby give a market advantage to the competition of those countries.

(f) The Westinghouse capacity to invest corporate assets in research and development depends upon the success in obtaining and maintaining a competitive advantage.

(iii) The information is being transmitted to the Commission in confidence and, under the provisions of 10CFR Section 2.790, it is to be received in confidence by the Commission.

(iv) The information sought to be protected is not available in public sources or available information has not been previously employed in the same original manner or method to the best of our knowledge and belief.

(v) Enclosed is Letter NTD-NRC-95-4594, November 10, 1995 being transmitted by Westinghouse Electric Corporation (W) letter and Application for Withholding Proprietary Information from Public Disclosure, Brian A. McIntyre (W), to Mr. T. R. Quay, Office of NRR. The proprietary information as submitted for use by Westinghouse Electric Corporation is in response to questions concerning the AP600 plant and the associated design certification application and is expected to be applicable in other licensee submittals in response to certain NRC requirements for justification of licensing advanced nuclear power plant designs.

This information is part of that which will enable Westinghouse to:

(a) Demonstrate the design and safety of the AP600 Passive Safety Systems.

(b) Establish applicable verification testing methods.

(c) Design Advanced Nuclear Power Plants that meet NRC requirements.

(d) Establish technical and licensing approaches for the AP600 that will ultimately result in a certified design.

(e) Assist customers in obtaining NRC approval for future plants.

Further this information has substantial commercial value as follows:

(a) Westinghouse plans to sell the use of similar information to its customers for purposes of meeting NRC requirements for advanced plant licenses.

(b) Westinghouse can sell support and defense of the technology to its customers in the licensing process.

Public disclosure of this proprietary information is likely to cause substantial harm to the competitive position of Westinghouse because it would enhance the ability of competitors to provide similar advanced nuclear power designs and licensing defense services for commercial power reactors without commensurate expenses. Also, public disclosure of the information would enable others to use the information to meet NRC requirements for licensing documentation without purchasing the right to use the information.

The development of the technology described in part by the information is the result of applying the results of many years of experience in an intensive Westinghouse effort and the expenditure of a considerable sum of money.

In order for competitors of Westinghouse to duplicate this information, similar technical programs would have to be performed and a significant manpower effort, having the requisite talent and experience, would have to be expended for developing analytical methods and receiving NRC approval for those methods.

Further the deponent sayeth not.

Attachment A to NTD-NRC-95-4594

Enclosed Responses to NRC Requests for Additional Information

Re: WCOBRA/TRAC Computer Code
440353
440356

Re: NOTRUMP Computer Code
440325
440435 (contains Westinghouse proprietary information)
440437
440465
440469
440472
440484
440505 (contains Westinghouse proprietary information)

Re: AP600 OSU Test Facility
480214
480215
480222
480244
480245
480252
480253
480254
480255
480256
480257
480259
480263
480264
480265
480266
480271

Enclosure 2 to Westinghouse Letter NTD-NRC-95-4594

(Non proprietary copy of Enclosure 1)

Question 440.325

Re: WCAP-14206 (NOTRUMP CAD)
On page 1-8, the PIRT for AP600 is identified in Table 1-1. This PIRT omits several key component phenomena. Please see the attached Table for a more thorough listing of the PIRT for AP600. Key components that are missing include:

Component
- o Downcomer/lower plenum
- o Makeup/letdown
- o Upper head/upper plenum
- o Cold legs
- o Sump
- o Containment (Interior and Exterior)

In addition to very limited PIRT listing, key phenomenological behavior are also missing for the majority of the components given in Table 1-1. Please see the attached Table for further identification of key phenomenological behaviors.

1a. Please include these additional PIRT items or explain and justify why they were omitted from Table 1-1.

1b. Also, please explain why the time phase in Table 1-1 omits the long term phase after IRWST injection when the sump is of particular importance. Again, see the attached Table for PIRT information regarding the long-term sump recirculation.

A thorough explanation for each of the PIRT items is also desired. For example, a very short discussion of noncondensible gas effects from the accumulators is given on Page 1-10, where it is stated that a noncondensible gas model is being considered for AP600. As noted in the attached Table, noncondensible gas phenomena affect many of the components in AP600, particularly in regard to heat transfer degradation and disruption of natural circulation which was not discussed. The lack of a noncondensible gas model is considered a major shortcoming of the NOTRUMP code since it is considered essential for prediction of AP600 performance following small breaks.

1c. If a noncondensible gas model is not included in NOTRUMP, please provide assessments with an alternate methodology containing a noncondensible gas model to either 1) justify an alternate means to capture noncondensible effects, or 2) show noncondensible effects are not important.

Multi-dimensional effects can occur in the downcomer, core, plenums, CMTs, and IRWST. Without a multi-dimensional model, simulation of multi-dimensional effects with a one-D model may not be adequately simulated with specialized nodalizations.

1d. If a multi-dimensional model is not included in NOTRUMP, please explain and justify its omission for the above components.

Response:

The small-break LOCA PIRT has been evolving from the initial PIRT which was included in the NOTRUMP CAD to the PIRT given in the NOTRUMP OSU and SPES preliminary validation reports. The additional PIRT components that were identified in the RAI which were applicable, were included in the NOTRUMP preliminary validation reports. Westinghouse has separated the transient into a small-break transient and the long term cooling portion of the transient. The small-break LOCA transient ends with stable IRWST injection. After that period, the transient becomes a long term cooling transient. Therefore, the containment and sump components are not included in a small-break LOCA PIRT since the containment acts as a boundary condition for the calculation, and the small-break portion of the calculation is over before the sump becomes an active component.

The PIRT table attached to RAI 440.325 also included several different phenomena for consideration as requested in the RAI. This PIRT, designated as the NRC PIRT, is attached as Table 1 from the RAI. The table includes several different transients in addition to the small-break LOCA transient which was the focus of the CAD. In addition, the transients which are listed across the top of the table such as " MSLB with ADS" and others are beyond design basis accidents, or are accidents which are not classified as small-break LOCA transients. The inclusion of these additional transients increases the number of phenomena and the number of components that would have to be examined if the table was only focused on the small-break LOCA. Table 1 from the RAI has been retyped as Table 2 with only the small-break LOCA portion of the table retained. Also, since the containment acts only as a boundary condition, those phenomena which were containment related were not included in the revised table (Table 2). Table 2 can now be compared to the PIRT presented in the SPES-2 preliminary validation report (1) which is given as Table 3. Comparing these two tables indicates that there are more similarities then differences, however, the NRC PIRT table (Table 2) lists additional phenomena as compared to the Westinghouse PIRT.

One phenomenon which appears on the NRC PIRT (Table 2) is the effects of non-condensible gases on the thermal-hydraulic performance of the different components. Non-condensible gases did appear on the Westinghouse PIRT as part of the ACCUMULATOR component since this was the source of the non-condensible gases rather than each individual component. The effects of the presence of non-condensible gases has been assessed in the SPES-2 (Reference 440.325-2) and OSU (Reference 440.325-3) Test Analysis (TAR) reports for the small-break LOCA transients which were simulated in these facilities. The accumulator nitrogen discharge at the end of accumulator injection was simulated in these experiments, and the nitrogen was discharged into the simulated reactor vessel through the DVI lines.

The time period when the Nitrogen discharge occurs is of importance in the AP600 design. For the small-break LOCA transient, the initial depressurization is caused by the break, then as the CMTs drain, the ADS is activated and the reactor system depressurizes below the accumulator set-point pressure of 700 psia. The accumulators are typically empty and discharge nitrogen at pressures in the range of 100 psia as seen in the SPES tests. At the time that the nitrogen (air in SPES-2) is injecting, the stages of ADS 1-3 either have opened or are in the process of opening. The ADS 1-3 then becomes the main energy release path and the PRHR becomes less important. The SPES-2 TAR, Reference 440.325-2, Pages 4.4-1 to 4.4-3 discusses the PRHR heat transfer and indicates that once the larger ADS 1-3 valves open, the heat removal from the PRHR significantly decreases. This PRHR energy removal decrease occurs before the air from the accumulators is injected. There is evidence from some of the SPES tests that the air does reach the cold leg balance line and is collected in the CMTs. This poses no problem since the presence of air would reduce any condensation in the CMTs and would allow them to drain more freely. Air is also believed to reach the PRHR, but it appears to only have a secondary effect on the PRHR performance. Again, this occurs at a time when the energy removal from the PRHR is small relative to the larger break caused by the ADS stages 1-3. The analysis of the OSU tests indicate that the effects of the nitrogen from the accumulators can not be detected in the experiment, see Reference (3), pages 6.1.4-1 to 6.1.4-2. The levels in the vessel were higher in the OSU tests such that the majority of the nitrogen was believed to be forced out the break. There was no evidence of the nitrogen in the CMTs or affecting the PRHR.

Therefore, since the experimental evidence indicates that the effects of non-condensible gases had little to no effect on the component thermal-hydraulic behavior, the non-condensible phenomena was dropped from the final PIRT.

In the NRC PIRT (Table 2) there are also phenomena which would be of interest if a coupled primary system calculation and a containment calculation were being performed simultaneously. These include the energy release phenomena as listed under the ADS and break components, as well as the containment and sump response. There are also phenomena which do not refer specifically to the small-break LOCA and are left blank in the small-break LOCA portion of the table. These phenomena can be deleted for the small-break LOCA portion of the transient. These include boron reactivity feedback and moderator feedback for the fuel rod component, condensation in the pressurizer, steam generator asymmetric behavior, and steam generator energy release and mass flow.

There are also areas where the Westinghouse PIRT is more complete then the NRC PIRT, particularly in the steam generator area. Also, the Westinghouse PIRT has four time periods while the NRC PIRT has five. The NRC "passive decay heat removal and the CMT draining to ADS actuation" period is the same as the Westinghouse PIRT time period called "natural circulation" during which the primary system is in single phase and two-phase natural circulation as the system drains. The natural circulation of the CMT and the PRHR is also considered during this time period. Therefore, combining these two time periods and the remaining NRC phenomena and the Westinghouse PIRT, a final PIRT can be developed for the AP600 small-break LOCA which contains the key aspects of both original PIRTS. The final PIRT is given in Table 4. Also included in the final PIRT are the specific thermal/hydraulic phenomena identified in the CMT separate effects tests and the ADS tests. The phenomena in the PIRT capture both the NRC and the Westinghouse identified phenomena. The rankings of the phenomena done by Westinghouse are not significantly different then the rankings used by the NRC.

Those specific items which pertain to the AP600 Small-break LOCA have been added to the final Westinghouse small-break LOCA PIRT as given in Table 4. The long term cooling portion of the NRC PIRT has been dropped since it does not directly pertain to the small-break LOCA portion of the transient and the review of the NOTRUMP Code Applicability Document since NOTRUMP is not used for the long term cooling calculations.

NOTRUMP does not have a non-condensible gas model, although the heat transfer could be degraded to account for the non-condensible effects if needed. The above discussion indicated that the effects of non-condensible gases were not observed in the SPES and OSU experiments. Also, the timing of the gas release from the accumulators is important since the gas is released after the larger ADS 1-3 valves open and the more rapid depressurization has begun. Once the larger ADS valves open, the main energy release path is from the ADS and the energy release from the PRHR decreases. This was observed in the SPES and OSU experiments. Therefore, the effects of noncondensibles are not significant for the AP600 system performance and do not need to be modeled in the NOTRUMP code.

The small-break LOCA transient is a quasi-steady state transient which occurs over hundreds to thousands of seconds as compared to a large break LOCA transient which lasts only 100 to 200 seconds. The dynamic effects in a small-break are significantly reduced from the large break since the reactor system is slowly draining out the break while the flows are circulating due to natural circulation and the core is a boiling pot. Therefore, since strong flows and pressure forces do not exist, and since the majority of the system is at the saturation temperature there is no need for three-dimensional modeling in the primary system. For areas where strong temperature gradients can exist such as in the CMTs and IRWST, one-dimensional modeling is adequate. The CMT test data (4) shows that the CMT will axially stratify. The PRHR tests also indicate that the IRWST will also axially stratify such that one-dimensional modeling is adequate.

SSAR Revision: NONE

References:

440.325-1 Meyer, P. E., Graziosi, G., Gonzalas, J., Kester, D. A., Saunders, S. E., and L. E. Hochreiter, "NOTRUMP Preliminary Validation Report for SPES-2 Tests," PXS-GSR-002, (July 1995)

440.325-2 Cunningham, J. P., Friend, M. T., Hochreiter, L. E., Hundal, R., Merritt, V., Ogrinsh, M., and R. F. Wright, "AP600 SPES-2 Test Analysis Report," WCAP-14254, (May 1995)

440.325-3 Andreychek, T. S., Chismar, S. A., Delose, F., Fanto, S. V., Fittante, R. L., Frepoli, C., Friend, M. T., Haberstroh, R. C., Hochreiter L. E., Morrison, W. R., Ogrinsh, M., Peters, F. E., Wright, R. F., and H. C. Yeh, "AP600 Low Pressure Integral Systems Tests at Oregon State University Test Analysis Report," WCAP-14292, (September 1995)

440.325-4 Cunningham, J. P., Haberstroh, R. C., Hochreiter, L. E., and R. F. Wright, "AP600 Core Makeup Tank Test Analysis," WCAP-14215 (December 1994)

TABLE 1
NRC PIRT TABLE

Component	Phenomena	SBLOCA					MSLB w/o ADS		MSLB with ADS					SGTR w/o ADS		SGTR with ADS				
		1	2	3	4	5	1	2	1	2	3	4	5	1	2	1	2	3	4	5
Accumulators	Flow			M	H							H							H	
	Noncondensible effects			L	M							M							M	
ADS	Energy release				H	H						H	H						H	H
	Mass flow				H	H						H	H						H	H
	Flow resistance				M	M						M	M						M	M
	Noncondensible effects				M	L						M	L						M	L
Break	Choking in complex geometries													H	H	H	H	M	M	M
	Energy release	L	H	H	H	M	H		H					M	H	M	H	H	M	M
	Flow resistance				M		L		L					M	M	M	M	M	L	L
	Mass flow	H	H	H	H	M	H		H					H	H	H	H	H	M	M
	Noncondensible effects				M															
Cold legs	Condensation					L							L							L
	Flashing			L	L							L						L	L	
	Loop asymmetry effects		L	M			M		M		M							M		
	Noncondensible effects				M	L						L	L						L	L
	PBL-to-cold legs tee phase separation		H	H	M	L											H	H	L	
	Stored energy release		L		L		L		L			L			L		L		L	
Core	Core channeling						H	L	H	L										
	Flashing			L	M		M	M	M	M		M						L	M	
	Flow resistance		L	L		M		L		L	L		M		L		L	L		M
	Loop asymmetry effects																L	L		
	Mass flow, including bypass	L	L	L														L		
	Noncondensible effects						L		L	L										
	Stored energy release		L		L		L		L			L			L		L		L	
	Subcooling margin														M		M			

TABLE 1
NRC PIRT TABLE

Component	Phenomena	SBLOCA					MSLB	w/o ADS	MSLB with ADS					SGTR	w/o ADS	SGTR with ADS				
		1	2	3	4	5	1	2	1	2	3	4	5	1	2	1	2	3	4	5
	Two-phase mixture level				H	H						H	H						H	H
	Voiding						M	M	M	M										
CMT	CMT-to-loop differential density		H				L	L	L	M					M		H			
	Condensation			L							L							L		
	Flashing			L	L						L	L						M	L	
	Flow resistance		M	L				L		L	L				L		M	L		
	Level			H	H			M			H	H			M			H	H	
	Noncondensible effects						L	L	L	L										
	Thermal stratification		M	L	L		L		L	M	L	L			M		M	L	L	
	Voiding							L		L										
Downcomer/lower plenum	Condensation		M	M	L	M							M		L		L	L	L	M
	Flashing				L							L							L	
	Flow distribution			M				L		L	L									
	Level			L		H						L	H					L	L	H
	Loop asymmetry effects		M				M		M								M	M		
	Noncondensible effects				L							L							L	
	Stored energy release		L		L		L		L			L			L		L		L	
Fuel Rods	Boron reactivity feedback						L		M											
	CHF						M		M											
	Core power/decay heat	H	H	H	H	H	H	H	H	H	H	H	H	H	H	H	H	H	H	H
	Moderator temperature feedback						L		M											
	Stored energy release	L	L		L		L		L			L		L	L	L	L		L	
Hot legs	CCFL				M	M						M	M						M	M
	Countercurrent flow				M	M						M	M						M	M
	Entrainment				M							M							M	

TABLE 1
NRC PIRT TABLE

Component	Phenomena	SBLOCA					MSLB	w/o ADS	MSLB with ADS					SGTR	w/o ADS	SGTR with ADS				
		1	2	3	4	5	1	2	1	2	3	4	5	1	2	1	2	3	4	5
	Flashing		L	L	M		M		M		L	M			M		M	L	M	
	Horizontal fluid stratification			M	M	M					M	M	M					M	M	M
	Loop asymmetry effects		L				M		M						M		M			
	Noncondensible effects				L		L	M	L	M		L							L	
	Phase separation in tees			L	H	H		M		M	L	H	H					L	H	H
	Stored energy release		L		L		L		L		L	L			L		L		L	
	Voiding		M				M	M	M	M					M		M			
IRWST	Discharge line flashing					M							M							M
	Flow and temperature distribution in PRHR bundle region		M	M				M		M	M				M		M	M		
	Flow resistance					M							M							M
	Interphasic condensation		L	L	M			L		L	L	M			L		L	L	M	
	Pool flow		L	L	M			L		L	L	M			L		L	L	M	
	Pool level		M	M	L	M		M		M	M	L	M		M				L	M
	Pool to tank structure heat transfer				L	L						L	L						L	L
	Pool thermal stratification		M	M	M	M	L	M	L	M	M	M	M		M		M	M	M	M
Makeup/letdown systems	Net makeup flow													H	H	H	H	H		
Pressurizer	Condensation							L												
	CCFL				M							M							M	
	Entrainment/De-entrainment				M							M							M	
	Flashing	H	M				M		M					H	M	H	M			
	Heater power													H		H				
	Level (inventory)	H	L				M	M	M	M	M			H	M	H	M			
	Level swell				M							M							M	

TABLE 1
NRC PIRT TABLE

Component	Phenomena	SBLOCA					MSLB	w/o ADS	MSLB with ADS					SGTR	w/o ADS	SGTR with ADS				
		1	2	3	4	5	1	2	1	2	3	4	5	1	2	1	2	3	4	5
	Noncondensible effects				L		M	M	M	M		L		L	L	L	L		L	
	Stored energy release				L							L		L		L			L	
	Vapor space behavior	H					M	M	M	M				H		H				
PRHR	Condensation		M	M			M	M	M						M		M	M		
	Differential density		M	M	L		M	M	M	M	M	L			M		M	M	L	
	Flow resistance		M	M	L			M		M	M	L			M		M	M	L	
	Flashing				L							L							L	
	Heat transfer between PRHR and IRWST		H	H	M	L	M	H	M	H	H	M	L		H		H	H	M	L
	Noncondensible effects		M	M	L		M	M	M	M	M	L			M		M	M	L	
	Phase separation in tees				L							L							L	
	Voiding		M	M			M	M	M	M	M				M		M	M		
Pumps	Coastdown performance		L				H		H						L		L			
	Flow resistance		L	L			L	L	L	L	L				L		L	L		
Steam generators	Asymmetric behavior							M		M	M									
	Condensation in U-tubes		L	L											L		L	L		
	Noncondensible effects							M		M	M									
	Primary to secondary heat transfer	H	H	M	L	L		M		M	M	L	L	H	H	H	H	H	L	L
	Secondary level		L	L				L		L	L				M		M	M	L	L
	Secondary pressure		M	M				L		L	L			M	M	M	M	M	L	L
	SRV energy release													M	H	M	H	H		
	SRV mass flow													M	H	M	H	H		
	Tube voiding		M	M				M		M	M				M		M	M		
Steam generator (primary)	Noncondensible effects						L		L											
	Preferential loop cooldown						H		H											

TABLE 1
NRC PIRT TABLE

Component	Phenomena	SBLOCA					MSLB	w/o ADS	MSLB with ADS					SGTR	w/o ADS	SGTR with ADS				
		1	2	3	4	5	1	2	1	2	3	4	5	1	2	1	2	3	4	5
	Primary to secondary heat transfer						H		H											
	Thermal driving head						M		M											
	Voiding (unaffected loop)						M		M											
Steam generator (secondary)	Entrainment						H		H											
	Flashing (SG and feedwater line)						H		H											
	Level swell and depletion						H		H											
	Tube dryout (affected SG)						M		M											
Steam generator (separator/dryer)	Liquid carry-over						H		H											
Sump	Discharge line flashing					M							M							M
	Flow resistance					M							M							M
	Fluid temperature					M							M							M
	Level					M							M							M
Upper head/upper plenum	Entrainment/De-entrainment				M	H						M	H						M	H
	Flashing		L	L	M		M		M			M			M		M	L	M	
	Flow split (upper plenum)						M	M	M	M										
	Loop asymmetry effects		L				M		M						M		M			
	Stored energy release		L		L		L		L			L			L		L		L	
	Vapor space compression							M												
	Voiding						M	M	M	M	M								L	M
Containment (interior)	Condensate transport				L	M	L	M	L	L	L	L	M		M				L	M
	Condensation				M	M	L	M	L	L	L	M	M		M				M	M
	Interior to wall heat transfer				M	H	M	H	M	L	L	M	H		H				M	H
	Liquid distribution				L	M	L	M	L	L	L	L	M		M				L	M

TABLE 1
NRC PIRT TABLE

Component	Phenomena	SBLOCA					MSLB	w/o ADS	MSLB with ADS					SGTR	w/o ADS	SGTR with ADS				
		1	2	3	4	5	1	2	1	2	3	4	5	1	2	1	2	3	4	5
	Liquid holdup				L	M	L	M	L	L	L	L	M		M				L	M
	Natural convection				L	M	L	M	L	L	L	L	M		M				L	M
	Noncondensible effects				L	M	L	M	L	L	L	L	M		M				L	M
	Nonuniform steam/air distribution				L	M	L	M	L	L	L	L	M		M				L	M
	Noncondensible segregation				L	M	L	M	L	L	L	L	M		M				L	M
	Passive heat sink				M	M	M	M	M	L	L	M	M		M				M	M
	Steam-noncondensible mixing				L	M	L	M	L	L	L	L	M		M				L	M
Containment (exterior)	Air flow				L	M		M				L	M		M				L	M
	Atmospheric temperature				L	M		M				L	M		M				L	M
	Chimney effects				L	M		M				L	M		M				L	M
	Exterior to ambient heat transfer				M	H	L	H	L	L	L	M	H		H				M	H
	Humidity				L	M		M				L	M		M				L	M
	PCCS evaporation				M	M		M				M	M		M				M	M
	PCCS water flow				L	M		M				L	M		M				L	M
	PCCS wetting				L	M		M				L	M		M				L	M
	PCCS mixture convective heat transfer				L	M		M				L	M		M				L	M
	Radiation heat transfer				L	M		M				L	M		M				L	M

TABLE 2
NRC SBLOCA PIRT TABLE REVISED

Component	Phenomena	SBLOCA				
		1	2	3	4	5
Accumulators	Flow			M	H	
	Noncondensible effects			L	M	
ADS	Energy release				H	H
	Mass flow				H	H
	Flow resistance				M	M
	Noncondensible effects				M	L
Break	Choking in complex geometries					
	Energy release	L	H	H	H	M
	Flow resistance				M	
	Mass flow	H	H	H	H	M
	Noncondensible effects				M	
Cold legs	Condensation					L
	Flashing			L	L	
	Loop asymmetry effects		L	M		
	Noncondensible effects				M	L
	PBL-to-cold legs tee phase separation		H	H	M	L
	Stored energy release		L		L	
Core	Core channeling					
	Flashing			L	M	
	Flow resistance		L	L		M
	Loop asymmetry effects					
	Mass flow, including bypass	L	L	L		
	Noncondensible effects					
	Stored energy release		L		L	
	Subcooling margin					

TABLE 2
NRC SBLOCA PIRT TABLE REVISED

Component	Phenomena	SBLOCA				
		1	2	3	4	5
	Two-phase mixture level				H	H
	Voiding					
CMT	CMT-to-loop differential density		H			
	Condensation			L		
	Flashing			L	L	
	Flow resistance		M	L		
	Level			H	H	
	Noncondensible effects					
	Thermal stratification		M	L	L	
	Voiding					
Downcomer/lower plenum	Condensation		M	M	L	M
	Flashing				L	
	Flow distribution			M		
	Level			L		H
	Loop asymmetry effects		M			
	Noncondensible effects				L	
	Stored energy release		L		L	
Fuel Rods	Boron reactivity feedback					
	CHF					
	Core power/decay heat	H	H	H	H	H
	Moderator temperature feedback					
	Stored energy release	L	L		L	
Hot legs	CCFL				M	M
	Countercurrent flow				M	M
	Entrainment				M	
	Flashing		L	L	M	

TABLE 2
NRC SBLOCA PIRT TABLE REVISED

Component	Phenomena	SBLOCA				
		1	2	3	4	5
	Horizontal fluid stratification			M	M	M
	Loop asymmetry effects		L			
	Noncondensible effects				L	
	Phase separation in tees			L	H	H
	Stored energy release		L		L	
	Voiding		M			
IRWST	Discharge line flashing					M
	Flow and temperature distribution in PRHR bundle region		M	M		
	Flow resistance					M
	Interphasic condensation		L	L	M	
	Pool flow		L	L	M	
	Pool level		M	M	L	M
	Pool to tank structure heat transfer				L	L
	Pool thermal stratification		M	M	M	M
Pressure	Condensation					
	CCFL				M	
	Entrainment/De-entrainment				M	
	Flashing	H	M			
	Heater power					
	Level (inventory)	H	L			
	Level swell				M	
	Noncondensible effects				L	
	Stored energy release				L	
	Vapor space behavior	H				

TABLE 2
NRC SBLOCA PIRT TABLE REVISED

Component	Phenomena	SBLOCA				
		1	2	3	4	5
PRHR	Condensation		M	M		
	Differential density		M	M	L	
	Flow resistance		M	M	L	
	Flashing				L	
	Heat transfer between PRHR and IRWST		H	H	M	L
	Noncondensible effects		M	M	L	
	Phase separation in tees				L	
	Voiding		M	M		
Pumps	Coastdown performance		L			
	Flow resistance		L	L		
Steam generators	Asymmetric behavior					
	Condensation in U-tubes		L	L		
	Noncondensible effects					
	Primary to secondary heat transfer	H	H	M	L	L
	Secondary level		L	L		
	Secondary pressure		M	M		
	SRV energy release					
	SRV mass flow					
	Tube voiding		M	M		
Steam generator (primary)	Noncondensible effects					
	Preferential loop cooldown					
	Primary to secondary heat transfer					
	Thermal driving head					
	Voiding (unaffected loop)					
Steam generator (secondary)	Entrainment					
	Flashing (SG and feedwater line)					

TABLE 2
NRC SBLOCA PIRT TABLE REVISED

Component	Phenomena	SBLOCA				
		1	2	3	4	5
	Level swell and depletion					
	Tube dryout (affected SG)					
Sump	Discharge line flashing					M
	Flow resistance					M
	Fluid temperature					M
	Level					M
Upper head/upper plenum	Entrainment/De-entrainment				M	H
	Flashing		L	L	M	
	Flow split (upper plenum)					
	Loop asymmetry effects		L			
	Stored energy release		L		L	
	Vapor space compression					
	Voiding					

TABLE 3
WESTINGHOUSE PHENOMENA IDENTIFICATION RANKING TABLE FOR AP600 SMALL-BREAK LOCA

Component Phenomenon	Blowdown	Natural Circulation	ADS Blowdown	IRWST Injection Cooling
Break				
Critical Flow	H	H	H	M
Subsonic Flow	N/A	N/A	N/A	M
ADS Stages 1 to 3				
Critical Flow	H* (inadvertent ADS)	H* (inadvertent ADS)	H	M
Two-Phase Pressure Drop	N/A*	N/A*	H	M
Valve Loss Coefficients	N/A*	N/A*	H	M
Single-Phase Pressure Drop	N/A	N/A	N/A	L
Vessel/Core				
Decay Heat	H	H	H	H
Forced Convection	M	N/A	N/A	N/A
Flashing	M	N/A	M	L
Wall Stored Energy	M	N/A	M	M
Natural Circulation Flow and Heat Transfer	M	M	M	M
Mixture Level Mass Inventory	H	H	H	H
RCP				
RCP Performance	M	N/A	N/A	N/A
Pressurizer				
Pressurizer Fluid Level	M	M	M	L
Wall Stored Heat	M	M	M	L
Pressurizer Surge Line				
Pressure Drop/Flow Regime	L	L	M	L
Downcomer/Lower Plenum	L	M	M	M
Upper Head/Upper Plenum	L	M	M	M
Cold Legs	L	M	M	M

TABLE 3
WESTINGHOUSE PHENOMENA IDENTIFICATION RANKING TABLE FOR AP600 SMALL-BREAK LOCA

Component Phenomenon	Blowdown	Natural Circulation	ADS Blowdown	IRWST Injection Cooling
Steam Generator				
2ϕ - Natural Circulation	L	M	L	L
Steam Generator Heat Transfer	L	M	L	L
Secondary Conditions	L	M	L	L
Hot Leg				
Flow Pattern Transition	L	H	H	H
ADS 1-4				
Critical Flow	N/A	N/A	H	H
Subsonic Flow	N/A	N/A	L	H
CMT				
Recirculation Injection	M	M	L	L
Gravity Draining Injection	N/A	M	H	L
Vapor Condensation Rate	N/A	M	M	L
CMT Balance Lines				
Pressure Drop	M	H	H	L
Flow Composition	M	H	H	L
Accumulators				
Injection Flow Rate	N/A	M	H	N/A
Noncondensible Gas Entrainment	N/A	N/A	L	L
IRWST				
Gravity Draining Injection	N/A	N/A	N/A	H
Vapor Condensation Rate	N/A	N/A	M	L
DVI Line				
Pressure Drop	M	M	M	M
PRHR				
Natural Circulation Flow and Heat Transfer	L	H	M	L

Notes:

H - High Importance, M - Moderate Importance, L - Low Importance, N/A - Not Applicable

The ADS is not normally opened during these phases unless the transient is an inadvertent ADS; in that case, the ADS phenomena would be ranked as high (H).

TABLE 4
WESTINGHOUSE FINAL PIRT FOR AP600 SBLOCA

Component Phenomenon	Blowdown	Natural Circulation	ADS Blowdown	IRWST Injection Cooling
ADS Stages 1-3				
Critical Flow	H* (inadvertent ADS)	H* (inadvertent ADS)	H	L
Two-Phase Pressure Drop	N/A*	N/A*	H	L
Valve Loss Coefficients	N/A*	N/A*	H	L
Single-Phase Pressure Drop	N/A	N/A	N/A	L
ADS 1-4				
Critical Flow	N/A	N/A	H	L
Subsonic Flow	N/A	N/A	L	M
Two-phase pressure drop	N/A	N/A	M	M
Break				
Line Resistance	N/A	N/A	L	L
Critical Flow (in complex Geometries)	H	H	H	N/A
Subsonic Flow	N/A	N/A	L	L
Discharge Coefficient	M	M	L	L
Accumulators				
Injection Flow Rate	N/A	M	H	N/A
Noncondensible Gas Entrainment	N/A	N/A	L	L
Cold Legs				
Flashing	N/A	N/A	L	N/A
PBL-to-Cold Leg Tee	N/A	H	H	L
Phase Separation	N/A	H	H	L
Stored Energy Release	N/A	L	N/A	L
Vessel/Core				
Decay Heat	H	H	H	H
Forced Convection	M	N/A	N/A	N/A
Flashing	M	N/A	M	L
Wall Stored Energy	M	N/A	M	M
Natural Circulation Flow and Heat Transfer	M	M	M	M
Mixture Level Mass Inventory	H	H	H	H
Mass Flow	M	M	L	L
Flow Resistance	L	L	L	L
CMT Draining Effects				
Condensation on cold thick steel surfaces	N/A	N/A	M	N/A

TABLE 4
WESTINGHOUSE FINAL PIRT FOR AP600 SBLOCA

Component Phenomenon	Blowdown	Natural Circulation	ADS Blowdown	IRWST Injection Cooling
Transient conduction in CMT walls	L	L	M	N/A
Interfacial condensation on CMT water surface (break size dependent)	N/A	N/A	H	N/A
Dynamic effects of steam injection and mixing with CMT liquid and condensate	N/A	N/A	H	N/A
Thermal stratification and mixing of warmer condensate with colder CMT water	L	H	H	N/A
CMT Recirculation				
Natural circulation of CMT and CL balance leg	H	H	N/A	N/A
Liquid mixing of CL balance leg, condensate, and CMT liquid	H	H	N/A	N/A
Flashing effects of hot CMT liquid layer	N/A	L	M	N/A
CMT wall heat transfer	L	M	M	N/A
CMT Balance Lines				
Pressure Drop	M	H	H	N/A
Flow Composition	M	H	H	N/A
Downcomer/Lower Plenum				
Flashing	N/A	N/A	L	N/A
Level	M	M	H	H
Loop Asymmetry Effects	M	M	L	L
Stored Energy Release	L	L	L	L
Hot Legs				
Countercurrent Flow	N/A	L	L	N/A
Entrainment	L	L	M	M
Flashing	L	L	L	N/A
Horizontal Fluid Stratification	N/A	M	M	M
Phase Separation in Tees (Flow Region)	N/A	M	M	M
IRWST				
Discharge Line Flashing	N/A	N/A	N/A	N/A
Flow and Temperature Distribution in PRHR Bundle Region	L	M	L	N/A
Pool Level	N/A	M	L	H
Gravity Draining	N/A	N/A	N/A	H
Vapor Condensation	N/A	M	M	L

TABLE 4
WESTINGHOUSE FINAL PIRT FOR AP600 SBLOCA

Component Phenomenon	Blowdown	Natural Circulation	ADS Blowdown	IRWST Injection Cooling
DVI Line Pressure Drop (Flow Resistance)	M	M	M	M
Pressurizer CCFL	N/A	N/A	M	N/A
Entrainment/De-entrainment	N/A	N/A	M	N/A
Flashing	H	N/A	M	N/A
Level (Inventory)	M	M	M	N/A
Level Swell	M	L	M	N/A
Stored Energy Release	L	L	L	N/A
Vapor Space Behavior	N/A	N/A	L	N/A
Pressurizer Surge Line Pressure Drop	L	L	M	N/A
Flooding	L	L	M	N/A
Steam Generator 2φ - Natural Circulation	M	M	N/A	N/A
Steam Generator Heat Transfer	M	M	L	N/A
Secondary Conditions	L	M	L	N/A
U-tube Condensation	L	L	N/A	N/A
Secondary Level	L	M	N/A	N/A
Secondary Pressure	M	M	N/A	N/A
Steam Generator Tube Draining	L	M	N/A	N/A
PRHR 1φ Heat Transfer	M	M	N/A	N/A
2φ Heat Transfer Condensation	N/A	M	L	N/A
Non-Condensible Gas Effects	N/A	N/A	L	N/A
Recirculation Flow	M	M	L	N/A
Upper Head/Upper Plenum				
Draining Effects	L	M	M	N/A
Flashing	L	N/A	M	N/A
Mixture Level	H	H	H	H
Entrainment/Deentrainment	N/A	L	M	M

TABLE 4
WESTINGHOUSE FINAL PIRT FOR AP600 SBLOCA

Component Phenomenon	Blowdown	Natural Circulation	ADS Blowdown	IRWST Injection Cooling
RCP				
Coast Down	L	N/A	N/A	N/A
Flow Resistance	L	L	N/A	N/A

Question 440.353

Re: WCAP-14171 (WCOBRA/TRAC CAD)
Once the accumulator empties, AP600 will depend on hydrostatic forces for further ECC makeup flow. There may be problems with core makeup tank (CMT) draining due to interference by condensation-related effects. Condensation of steam flowing in from the cold leg/CMT pressure balance line (PBL) will occur on the cold CMT water. This condensation may affect CMT draining; therefore, accurate modeling of interphase heat and mass transfer is crucial to the successful prediction of CMT injection. Describe the tests that will be or were used to assess this phenomena as it applies to CMT draining. Provide comparisons between the test data and WCOBRA/TRAC calculations to demonstrate the code is capable of correctly modeling CMT draining in the presence of condensation.

Response:

The condensation of balance line steam is a significant factor in determining the rate of flow of water out of the CMTs. For this reason, testing was performed at the Core Makeup Tank test facility as reported in Reference 440.353-1. In the 300 series tests, a 1/6th diameter scale CMT was tested for large break LOCA conditions in which water was allowed to drain from the bottom of the tank while steam flowed into the top of the tank. The steam replaced the volume of the draining water; some steam condensed on the cold surface of the water, and some condensed on the cold wall. The 300 series tests have been modelled by WCOBRA/TRAC, as reported in Reference 440.353-2, and the comparisons to the test data are provided in that document.. Acceptable agreement for drain rates from the CMT were obtained for the 300 series tests by the appropriate selection of the noding sizes in the CMT. This noding approach has been applied when performing the AP600 Preliminary SSAR large break LOCA and long-term cooling calculations with WCOBRA/TRAC (Reference 440.353-3). Additional justification for the CMT modelling is provided by the modelling of the Oregon State University tests (Reference 440.353-4), in which the same approach to noding the CMT was used and acceptable agreement was obtained for small break LOCA simulations extending into Long Term Cooling. Reference 440.353- 2 assesses the CMT drain rate sensitivity to the heat transfer coefficient assumed at CMT wall surfaces. Together, References 440.353-2 and 4 demonstrate that WCOBRA/TRAC adequately models the steam/water condensation and mixing which occur in the core makeup tanks during the various phases of postulated LOCAs in the AP600.

References:

440.353-1 Leonelli K, "Core Makeup Tank Test Data Report", WCAP-14217 (proprietary), November, 1994.

440.353-2 Haberstroh R C, Hochreiter L E and Monahan E M, "WCOBRA/TRAC Core Makeup Tank Preliminary Validation Report",MT-01-GSR003, February, 1995.

440.353-3 Letter NTD-NRC-95-4480, "Preliminary Marked Up Sections of SSAR Chapter 15, Revision 5", June 2, 1995

440.353-4 Chow S K et al, "WCOBRA/TRAC OSU Long Term Cooling Preliminary Validation Report" LTCT-GSR-003, September 1995.

SSAR Revision: NONE

Question 440.356

Re: WCAP-14171 (WCOBRA/TRAC CAD)
Long term cooling results from gravity drained systems with low driving heads in the presence of competing forces. Long term cooling was not addressed in the WCOBRA/TRAC CQD; therefore, describe the LTC methodology (if it uses WCOBRA/TRAC), describe how the LTC methodology will be verified, and compare WCOBRA/TRAC results with the assessment data to demonstrate code performance in this area.

Response:

The Long Term Cooling (LTC) phase of the transient begins at the start of the IRWST injection and continues to the end of the transient. The WCOBRA/TRAC methodology for LTC takes into account that the AP600 small break LOCA and LTC transients can extend for very long time periods (typically 5 to 24 hours), by which time there is sustained, stable injection from the sump into the reactor vessel. While long simulations are possible with WCOBRA/TRAC, they are not practical due to the extreme computer running times that are necessary. The approach used for the SSAR analysis is to perform the LTC calculations in a "window" mode. This means that the WCOBRA/TRAC long term cooling calculation is started at a given point during the long term transient with conditions that either come from a previous WCOBRA/TRAC large-break LOCA calculation or from a NOTRUMP small-break LOCA calculation, or are reasonable estimates of the primary system inventory at the time of the calculation. The long term cooling calculation proceeds for approximately 1000 seconds to verify that the passive safety injection system is providing sufficient flow into the reactor vessel, and to show positive liquid flow through the core which precludes boron precipitation.

The OSU experiments were used to validate WCOBRA/TRAC for long term cooling for both the initial portion of the small break LOCA transient and the window mode of the long term phase of LOCA transients. The approach used in modelling the OSU tests to validate the WCOBRA/TRAC LTC methodology (Reference 440.356-1) was two-fold:

The small break LOCA period is modelled with WCOBRA/TRAC so that the initial blowdown, natural circulation, ADS blowdown and early IRWST injection phenomena of the test are calculated.

The simulation of the IRWST early injection phase provides the representative initial conditions to be used in a window mode simulation for later phases of the IRWST injection as well as the transition to sump injection. The window mode simulation is a series of quasi-equilibrium calculations, using WCOBRA/TRAC, over a selected time interval during the overall transient.

The other initial and boundary conditions required for the window mode simulations, which are taken from the test data, are the temperatures and water levels of the sump and IRWST and the core decay power. More details of the LTC methodology and its verification may be found in Reference 440.356-1.

The objective of the window mode simulation in Reference 440.356-2 is to show that the core remains covered during IRWST injection. The philosophy of the window mode approach is that during the early part of the window mode simulation, the impact of the assumed initial conditions decay so that they no longer influence the predicted results when the quasi- equilibrium condition for that window is achieved. The "window" mode calculations examine times when the passive safety systems are most challenged in terms of maintaining sufficient inventory in the reactor vessel such that the core does not heat-up. The first cases examined are the long term cooling behavior following a large-break LOCA. This transient was chosen since the core decay power is the largest when the reactor system transitions into long term cooling. The first window examines the cooling mode of the core with IRWST injection after the CMTs have ended injection, which occurs when the decay power is large. The single failure assumption is one fourth stage ADS valve fails to open. The second window examines the switch-over from IRWST injection to sump injection. The sump injection has a reduced head of water to drive the flow into the vessel, and the sump liquid is at an elevated temperature. The window calculation for the sump injection following the large-break LOCA maximizes the decay power in the core that the sump injection must cool. These two calculations bound most of the small break and large break transients. A third calculation performed in Reference 440.356-2 is initiated based on the NOTRUMP conditions following a small-break LOCA (2-inch cold leg break) in which the IRWST will have heated to a very high (saturated) temperature due to the heat transfer from the PRHR and the ADS. The window mode calculation bounds the sump injection initiation time of this transient and consitutes a bounding case for LTC following a small break LOCA by analyzing non-coincident worst conditions.

To validate the WCOBRA/TRAC code for the LTC transient, four different OSU tests were simulated and examined:

SB01 - 2 inch CL break test. This is the reference test.

SB10 - double-ended balance line break test. This is a small break test similar to but larger than SB01. There is also asymmetric CMT behavior.

SB12 - double-ended DVI line break test. Sump injection begins early in time when the core decay power is still high and steaming rates are large.

SB21 - simulated 4 inch breaks at the top and bottom of the CL-3. Rapid blowdown is achieved with early IRWST and sump injection at high core decay powers. The breaks on the top and bottom of the broken CL are similar to a circumferential split.

These tests capture the thermal hydraulic phenomena of interest for small breaks and LTC and validate the performance of WCOBRA/TRAC. This work is reported in Reference 440.356-1. The window modes selected include the start of sump injection; this period has a low flow rate and a high temperature in the DVI lines and the highest core power of the sump injection period. The window mode simulations for tests SB01, SB10 and SB21 start 200 seconds before the start of sump injection and run for (typically) 1000 seconds. In the case of test SB12, the window selected is the final 1000 seconds of IRWST injection. The first 400 seconds of each simulation are considered to be the period over which the WCOBRA/TRAC solution is approaching a quasi-equilibrium state. Average values used for comparison to the test data are taken from the period 400 seconds after the start of the window until the end of the window being simulated. A PIRT for Long Term Cooling is given in Reference 440.356-1 and is used as the basis for the assessment of the OSU predictions. The predictions are shown to be acceptable.

The containment pressure used in the Reference 440.354-2 analysis is obtained from AP600 WGOTHIC calculations. WGOTHIC is a state-of-the-art containment analysis tool which has been equipped with special models of the passive cooling mechanisms applicable to the AP600.

The OSU test program results (Reference 440.356-3), the WCOBRA/TRAC simulations of the OSU tests (Reference 440.356-1) and the SSAR LTC analyses provide confidence that the AP600 passive safety injection systems provide sufficient flow that the core will be safely cooled for an indefinite period following any postulated LOCA event.

References

440.356-1 Chow S K et al, "WCOBRA/TRAC OSU Long Term Cooling Preliminary Validation Report" LTCT-GSR-003

440.356-2 Letter NTD-NRC-95-4503, "Preliminary Marked Up Sections of SSAR Chapter 15, Revision 5", July 10, 1995

440.356-3 Dumsday C L et al, "AP600 Low Pressure Integral Systems Test at Oregon State University, Final Data report", WCAP-14252, May, 1995.

SSAR Revision: NONE

Question 440.435

Re: NOTRUMP ADS PVR (RCS-GSR-003)
The flow quality data show an increase in quality within the first six seconds for all of the tests while NOTRUMP displays a decreasing trend. While the flow quality at the sparger discharge will establish the depressurization rate for the system, the miscalculated flow quality, particularly in the beginning of each test, suggests that NOTRUMP is lacking dynamic effects. As such, explain how the two-region fluid model void distribution in the liquid regions is computed, and how this lower region void fraction affects the quality exiting a volume. Also, does the assumption that steam regions form above liquid regions affect the fluid void distribution in the ADS lines? That is, explain the conditions where separation occurs versus highly dispersed liquid-steam mixture conditions with void gradients and how NOTRUMP treats these conditions in the ADS lines. Are void gradients computed in the liquid regions? How is the release of steam from the liquid region computed; is it based on the average void fraction in the region or is a surface void fraction computed for release calculations? In vertical sections, during depressurization transients or vertical regions with high heat addition, large void gradients can develop where the surface void fractions can be two to three times greater than the average. Please explain how NOTRUMP treats the void distribution and release of steam from the two-phase regions under these conditions?

Response:

The large difference between the NOTRUMP calculated flow quality and the quality calculated from data in the first six seconds is due to the fact that there was a time delay in opening the VLI-1 valve. When the time is adjusted so that the comparison is based on a consistent VLI-1 valve opening time, the agreement is much better as discussed below.

Figures 440.435-1 and 440.435-2 show that in ADS Test 240 both the pressure and the mass in the supply tank are constant in the first 3.5 seconds, then decrease after 3.5 seconds. This means that VLI-1 gate valve did not open at time zero, rather it actually opened at 3.5 seconds. There are many reasons for this. First, the valve was initially very tightly closed. Therefore, when the power was applied to the gate valve, it took a period of time before the valve began to move. After the valve began to move, it took additional time to clear the seat and actually open sufficiently to allow flow to pass. Because of the shape of the gate valve, the valve opening area did not increase linearly at first, but increased very slowly, then gradually increases linearly increase as can be seen in figure 440.435-3. This is reflected in the pressure plot (Figure 440.435-1) and mass plot (Figure 440.435-2), where the curves change gradually, instead of sharply changing, at 3.5 seconds when the valve is open.

In the NOTRUMP simulation, the valve is assumed to open linearly from the time zero. To have a comparison between the NOTRUMP calculations and the data, it is necessary to find the effective opening time of the valve in the test. This is accomplished by intersecting the linear portion of the pressure curve (Figure 440.435-1) with the initial horizontal line, which is 3.5 seconds. Therefore, the comparison of Test 240 in reference 440.435-1 should be corrected by shifting the data curves to the left by 3.5 seconds so that the actual VLI-1 valve opening time is at time zero. The results are shown in Figures 440.435-4 through 440.435-13 (The original unshifted plots in reference 440.435-1 are shown following each shifted plot). It is seen that the agreement between the NOTRUMP calculated quality and the quality calculated from the data is much better. A similar time shift is applicable to other tests.

In the NOTRUMP model of the ADS tests, the homogeneous fluid model is used for all pipes. The two-region fluid model is used only for the supply tank, and not for pipes.

REFERENCE

440.435-1 Yeh, H. C. and L. E. Hochreiter, AP600 NOTRUMP Automatic Depressurization System Preliminary Validation Report, Westinghouse Electric Corporation, RCS-GSR-003, 1995.

440.435-2 Final Data Report for ADS Phase B1 Tests, WCAP-14324, April, 1995.

SSAR Revision: NONE

(a,b)

Figure 440.435-1 Supply Tank Pressure.

[ ](a,b)

Figure 440.435-2 Supply Tank Mass (Reference 440.435-2)

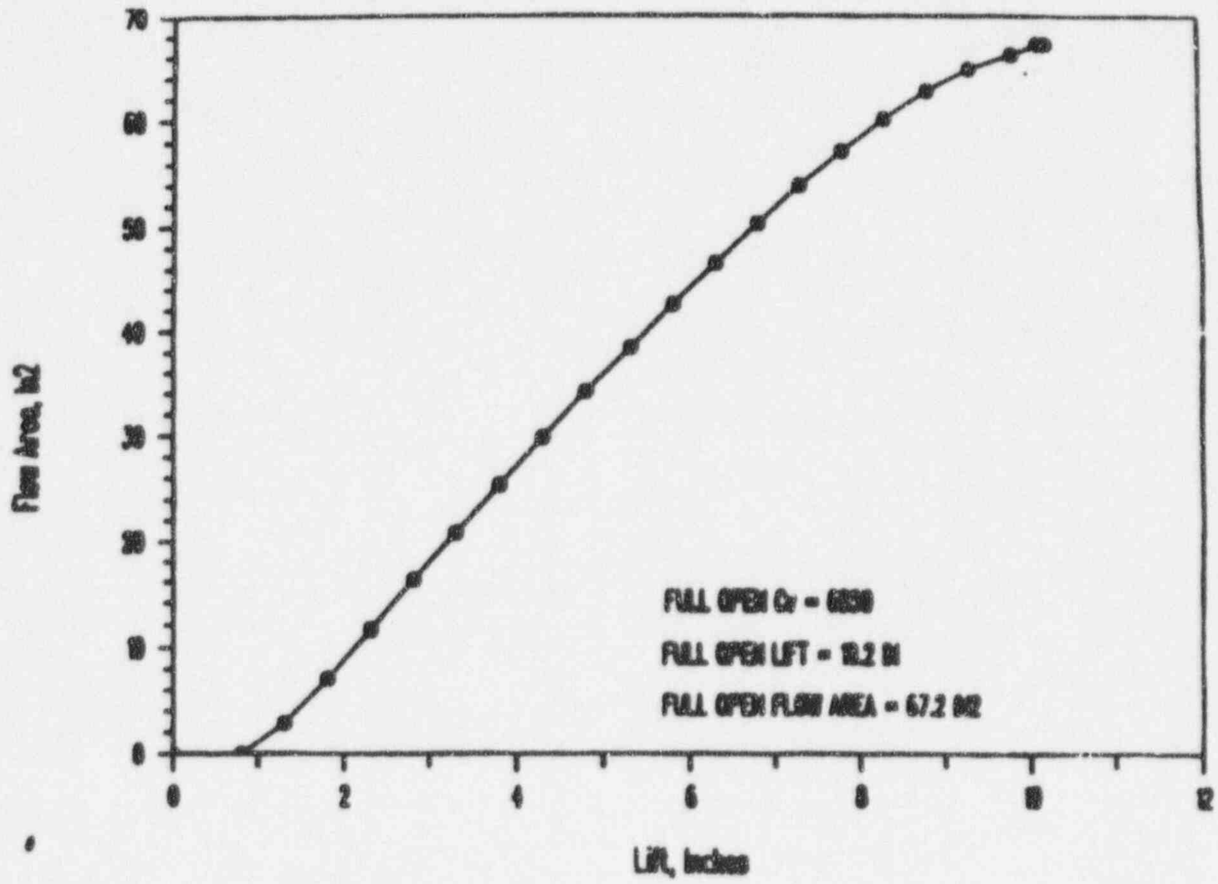

Figure 440.435-3 Valve opening Area As a Function of the Stem Travel for VLI-1 (Reference 440.435-2)

(a,b)

Figure 440.435-4 Comparison of the Quality Calculated by NOTRUMP and the Data Upstream of VLI-2 (A & M) Valve (Test 240). The time for the data curve has been shifted to the left for 3.5 seconds so that the time zero is the actual opening time of the valve VLI-1.

[ ]$^{(a,b)}$

Figure 440.435-5 The Original Unshifted Plot of Figure 440.435-4. (Figure 4-27 of Reference 440.435-1)

(a,b)

Figure 440.435-6 **Comparison of the Quality Calculated by NOTRUMP and the Data Upstream of the ADS Valves (PT6W)(Test 240). The time for the data curve has been shifted to the left for 3.5 seconds so that the time zero is the actual opening time of the valve VLI-1.**

[ ](a,b)

Figure 440.435-7 **The Original Unshifted Plot of Figure 440.435-6. (Figure 4-28 of Reference 440.435-1)**

(a,b)

Figure 440.435-8 Comparison of the Quality Calculated by NOTRUMP and the Data Downstream of the ADS Valves (PT16W)(Test 240). The time for the data curve has been shifted to the left for 3.5 seconds so that the time zero is the actual opening time of the valve VLI-1.

[ ](a,b)

Figure 440.435-9 The Original Unshifted Plot of Figure 440.435-8. (Figure 4-29 of Reference 440.435-1)

(a,b)

Figure 440.435-10 Comparison of the Quality Calculated by NOTRUMP and the Data at the Sparger Body (Test 240). The time for the data curve has been shifted to the left for 3.5 seconds so that the time zero is the actual opening time of the valve VLI-1.

(a,b)

Figure 440.435-11 The Original Unshifted Plot of Figure 440.435-10. (Figure 4-30 of Reference 440.435-1)

AP600

(a,b)

Figure 440.435-12 Comparison of the Quality Calculated by NOTRUMP and the Data at the Sparger Arms (Test 240). The time for the data curve has been shifted to the left for 3.5 seconds so that the time zero is the actual opening time of the valve VLI-1.

(a,b)

Figure 440.435-13 The Original Unshifted Plot of Figure 440.435-12. (Figure 4-31 of Reference 440.435-1)

Question 440.437

Re: NOTRUMP ADS PVR (RCS-GSR-003)
NOTRUMP overpredicts the depressurization rate in the pressurizer for several tests while the fluid qualities in the ADS lines for these tests were underpredicted. Since lower quality should lead to a reduced depressurization rate, please explain this inconsistency. See for example Figs. 4-13, and 4-33, 4-53. Also, these tests are only displayed for 30 seconds and only capture the very initial short period of the depressurization. Please explain why the comparisons were not carried out beyond 30 seconds or until atmospheric pressures are approached. Some of the tests show a marked deviation between the data and the NOTRUMP prediction suggesting the long term depressurization may be grossly overpredicted as in Figs. 4-53, while the flows show a growing discrepancy with the data as in Figs. 4-32 and 4-12 at 30 seconds. Since the ultimate judge of the ADS is its ability to depressurize the system to very low pressure, displaying the test comparisons for only the first 30 seconds where the system remains at elevated pressures does not demonstrate the NOTRUMP code ability to predict ADS depressurization over the full range of system pressures. Please provide the NOTRUMP comparisons to the data until the system has completely depressurized.

Response:
The depressurization of the pressurizer (steam/water supply tank) depends only the flow rate as analyzed and verified with the data below. The higher the flow rate, the higher the depressurization rate. NOTRUMP overpredicts the flow, therefore, it overpredicts the depressurization rate no matter the fluid qualities are underpredicted. There is no inconsistency.

To show that the depressurization of the pressurizer depends only on the flow rate but not on the fluid quality, consider the control volume enclosing the pressurizer volume as shown in Figure 440.437-1. The conservations of mass, energy, and pressurizer volume are:

$$(M_{g,0} + M_{f,0}) - (M_{g,t} + M_{f,t}) = \Delta M_{ST} = \int_0^t \dot{m}_{out}\, dt \qquad (440.437\text{-}1)$$

$$(M_{g,0}e_{g,0} + M_{f,0}e_{f,0}) - (M_{g,t}e_{g,t} + M_{f,t}e_{f,t})$$

$$= \int_0^t \dot{m}_{out}(H_f + K.E.)\, dt$$

$$= \Delta M_{ST}\frac{1}{2}(H_{f,0} + H_{f,t}) \qquad (440.437\text{-}2)$$

$$(M_{g,t}v_{g,t} + M_{f,t}v_{f,t}) = V_{ST} = (M_{g,0}v_{g,0} + M_{f,0}v_{f,0}) \qquad (440.437\text{-}3)$$

where: M = masses, lbm,
v = specific volume, ft^3/lbm,
e = internal energy, Btu/lbm,
H = enthalpy, Btu/lbm,
V = volume, ft^3,

$\dot{m}$ = mass flow rate, lbm/sec,

K.E. = kinetic energy, Btu/lbm.

Subscripts:
g = vapor,
f = liquid,
0 = time zero,
t = time t,
ST = pressurizer (steam/water supply tank).

In equation 440.437-2, the K.E. is neglected. Suppose that the initial mass and pressure in the pressurizer at time zero is given. Assume that the fluid is at saturation conditions initially and also later while flashing. That is, all the quantities with subscript 0 in the above three equations are known and the quantities with subscript t are unknown. Although there are many quantities with subscript t, in fact there are only three unknowns: $M_{g,t}$, $M_{f,t}$, and P_t. The pressure P_t is not explicitly in the three equations, however, all internal energies and enthalpies depend on P_t. That is, once P_t is found, the internal energies and enthalpies can be found from the steam table. Therefore, the three equations (1), (2), and (3) can be solved for the three unknowns $M_{g,t}$, $M_{f,t}$, and P_t if the flow rate $\dot{m}_{out}$ is known. That is, the pressure P_t depends only on the flow rate $\dot{m}_{out}$ and is independent of the fluid quality downstream. This can be verified by two methods: (a) substituting the time zero values and flow rate (or ΔM_{ST}) from test data in the above three equations, and solve the three equations for masses and pressure at time t, which involves iteration since the pressure does not explicitly appear in the equations, and showing that the calculated pressure at time t agrees with data; or alternatively, (b) substituting the time zero values and flow rate (or ΔM_{ST}) in the above three equations, and showing that the test data at time t satisfy the three equations. In the following calculations, the second method is used, since it is more straight forward and does not involve iteration.

ADS Test 240 is arbitraily chosen for verification of the above argument. The time zero values can be obtained from Table B.1-2 (p.B-9) of reference 440.437-1 as follows:

P_0 = 1202 psia, → $v_{f,0}$ = 0.02233 ft³/lbm , $v_{g,0}$ = 0.3617 ft³/lbm ,

$e_{f,0}$ = 567.1 Btu/lbm , $e_{g,0}$ = 1104.2 Btu/lbm ,

$H_{f,0}$ = 572.1 Btu/lbm , $\rho_{f,0}$ = 44.79 lbm/ft³

V_{ST} = 1412 ft³

$M_{g,0}$ = 1818 lbm

$(M_{f,0})_s$ = 26,476 lbm (see Figure 440.437-1)

ΔM_{ST} = 12055 lbm

What is needed in Equations 440.437-1, 440.437-2 and 440.437-3 is $M_{f,0}$, but not $(M_{f,0})_s$. The $M_{f,0}$ can be calculated as follows: (Note, V_{ST} = 1412 ft³, but we do not know V_b. We only know that V_b is approximately a hemispherical volume of $(4\pi/3)(6.98/2)^3$ = 178 ft³.)

$$V_{g,0} = M_{g,0} v_{g,0} = 1818\ (.3617) = 658\ \text{ft}^3$$

$$V_{f,0} = V_{ST} - V_{g,0} = 1412 - 658 = 754\ \text{ft}^3$$

$$M_{f,0} = V_{f,0}\ \rho_{f,0} = 754\ (44.79) = 33{,}772\ \text{lbm}$$

$$V_b = [\ M_{f,0} - (M_{f,0})_s\ ]\ /\ \rho_{f,0} = (33{,}772 - 26{,}476)\ /\ 44.79 = 163\ \text{ft}^3$$

Substituting these time zero values in equations (1), (2), and (3) with the neglect of the kinetic energy yields

$$M_{g,t} + M_{f,t} = (M_{g,0} + M_{f,0}) - \Delta M_{ST} = (1818 + 33{,}772) - 12055 = 23{,}535\ \text{lbm} \quad (440.437\text{-}4)$$

$$M_{g,t}\ e_{g,t} + M_{f,t}\ e_{f,t} = (M_{g,0} e_{g,0} + M_{f,0} e_{f,0}) - \Delta M_{ST} = [1818\ (1104.2) + 33{,}772\ (567.1)]$$

$$-12055\ (1/2)\ (572.1 + 556.7)$$

$$= 14.4 \times 10^6\ \text{Btu} \quad (440.437\text{-}5)$$

$$M_{g,t}\ v_{g,t} + M_{f,t}\ v_{f,t} = V_{ST} = 1412\ \text{lbm} \quad (440.437\text{-}6)$$

Since the data of $M_{g,t}$, $M_{f,t}$, ΔM_{ST}, and P_t at the end of test (35 seconds) are given in Table B.1-2 (page B-9) of reference 440.437-1, these data are used for time t (35 seconds) values. These data are

$t = 35$ sec.

$P_t = 1094$ psia $\rightarrow$ $v_{f,t} = 0.02193$ ft^3/lbm , $v_{g,t} = 0.4031$ ft^3/lbm ,

$e_{f,t} = 552.3$ Btu/lbm , $e_{g,t} = 1107.7$ Btu/lbm ,

$H_{f,t} = 556.7$ Btu/lbm

Substitute these data for time t values in equations (4) and (5), giving

$$M_{g,t} + M_{f,t} = 23{,}535 \qquad (440.437\text{-}7)$$

$$1107.7\ M_{g,t} + 552.3\ M_{f,t} = 14.4 \times 10^6 \qquad (440.437\text{-}8)$$

Equations (7) and (8) can be solved for $M_{g,t}$ and $M_{f,t}$:

$$M_{g,t} = 2{,}444 \qquad (440.437\text{-}9)$$

$$M_{f,t} = 21{,}091 \qquad (440.437\text{-}10)$$

Substituting equations (9) and (10) in the left-hand side of equation (6) gives

$$M_{g,t}\, v_{g,t} + M_{f,t}\, v_{f,t} = 2{,}444\ (0.4031) + 21{,}091\ (0.02193) = 1448\ \text{ft}^3$$

which is almost identical to the value on the right-hand side of equation (6), 1412 ft^3, with the error of only 2.5 percent. Thus, it is seen that the pressurizer pressure depends only on the total mass out of the pressurizer, ΔM_{ST}, and the depressurization rate depends only on the flow rate, $\dot{m}_{out}$. The larger the flow rate, $\dot{m}_{out}$, the larger the depressurization rate. Since NOTRUMP overpredicts the flow rate, it also overpredicts the depressurization rate, which is correct no matter what flow quality downstream is predicted.

In the six tests analyzed, the VLI-2 valve was closed at around 30 seconds because of the capacity of the steam/water supply tank (pressurizer) of the test facility. Therefore, the data after 30 seconds are meaningless and all figures in the report are displayed for 30 seconds. The NOTRUMP comparisons after 30 seconds are not valid since the test valve closure was not modeled with NOTRUMP.

Reference

440.437-1 WCAP-14324, "Final Data Report For ADS Phase B1 Tests," April 1995.

SSAR Revision: NONE

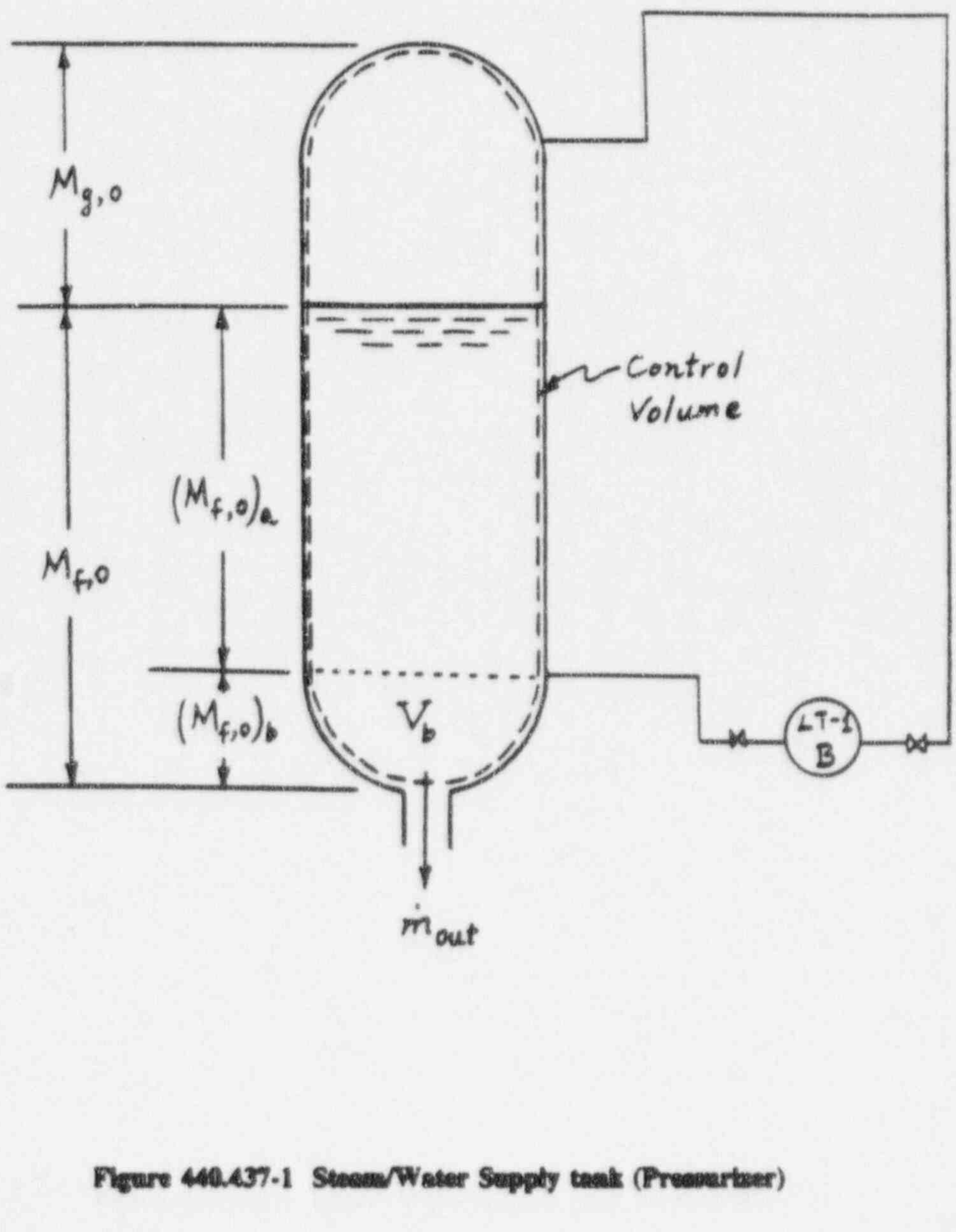

Figure 440.437-1 Steam/Water Supply tank (Pressurizer)

Westinghouse

Question 440.465

Re: NOTRUMP PVR FOR OSU TESTS, LTCT-GSR-001, JULY 1995
Fig. 2-2 shows the wall heat noding. Wall heat effects can represent a major source of heat for small break LOCAs which can subsequently affect depressurization, especially for the slow depressurization transients characterizing AP600 small break LOCA response. Please justify the omission of wall heat transfer from all of the external loop piping and the secondary system components.

Response:

Although the depressurization in the OSU facility small break LOCAs is slow, it is much more rapid than a standard PWR due to the ADS valves. In the OSU noding, the intent was to remain as faithful to the standard plant noding as possible, whenever it was reasonable to do so. In the OSU facility, the total metal mass of all hot and cold legs is only 340 lb. This accounts for only about 3% of the metal mass in the RCS. The more rapid AP600 depressurization, which is controlled by the ADS and not the break, places less importance on the metal heat contributions of the loop piping than in a standard PWR. The level of detail in the metal heat nodalization for standard PWRs was therefore deemed adequate for modelling the OSU facility.

SSAR Revision: NONE

Question 440.469

Re: NOTRUMP PVR FOR OSU TESTS, LTCT-GSR-001, JULY 1995
In expressing the momentum equations from a mass flow to a volumetric flow basis, linearizations of the equations are performed. Provide the volumetric flow based momentum equations and the linearizations that were performed to change the equations to a volumetric flow base. Provide the validations that were performed to verify that the changes were made correctly. Also, provide the code benchmark for this model change.

Response:

Following is the requested description. This description is in the form of a revision to Section 4.4 which will be included in the NOTRUMP Final V&V Report. Work is currently underway to respond to the request for validations and benchmark analyses. The schedule and scope of this work will be provided on or before 12/31/95.

4.4 Net Volumetric Flow-Based Momentum Equation

An option has been added to NOTRUMP to cast the momentum equation and drift flux equations for a given flow link in terms of net volumetric flow rate rather than net mass flow rate. The advantage of this modification is two-fold. First, having volumetric flow rate as the independent variable in a flow link allows the mass flow rate to change instantaneously as densities in the two adjacent nodes change. This improves the behavior of the node stacking and mixture-level tracking model, as well as the behavior of other flow links that experience large density gradients in time and space. It yields significant reductions in pressure oscillations, particularly at low pressures where the density differences between liquid and gas are the greatest. Second, drift flux models, in general, work better when cast in terms of net volumetric flow rate, since drift flux is a volumetric flow concept. The mass and energy equations are not directly impacted, since the drift flux model still gives, as its outputs, the phasic mass flow rates. Only the linearizations of these equations, with respect to the volumetric flow rate are changed and they are generally simpier than the current linearizations with respect to mass flow rates.

The mass flow-based momentum equation used in NOTRUMP is given by equation (2-33) of Reference 1. It is also written in a more general form as equation (2-38). Both of these equations are differential equations written in terms of the temporal derivative of the mass flow rate W. It is also possible to write these equations in terms of the temporal derivative of the volumetric flow rate Q. To do this refer to the drift flux equations in Appendix G of Reference 1. The equations for the phasic volumetric fluxes $<j_f>$ and $<j_g>$ in terms of the net (or total) mass flux G are

$$<j_f> = \frac{(1-<\alpha>C_o)\,G - \frac{<\alpha>}{\upsilon_g}<<V_{gj}>>}{\rho_m'} \qquad \text{(G-24)}$$

and

$$<j_g> = \frac{(<\alpha>C_o)\,G + \frac{<\alpha>}{\upsilon_f}<<V_{gj}>>}{\rho_m'} \qquad \text{(G-25)}$$

where

$$\rho_m^* = \frac{1-<\alpha>C_o}{\upsilon_f} + \frac{<\alpha>C_o}{\upsilon_g} \quad \text{(G-26)}$$

Adding equations (G-24) and (G-25) gives the following equation for the net volumetric flux <j> in terms of the net mass flux G.

$$<j> = \frac{G+\left(\frac{1}{\upsilon_f}-\frac{1}{\upsilon_g}\right)<\alpha> <<V_{gj}>>}{\rho_m^*} \quad \text{(4.4-1)}$$

Multiplying by the flow area A gives the following equation for the net volumetric flow rate Q in terms of the net mass flow rate W.

$$Q = \frac{W+\left(\frac{1}{\upsilon_f}-\frac{1}{\upsilon_g}\right)<\alpha> <<V_{gj}>>A}{\rho_m^*} \quad \text{(4.4-2)}$$

Differentiating equation (4.4-2) with respect to time t and neglecting the temporal derivatives of ρ_m^* and the second term in the numerator gives

$$\dot{Q} = \frac{\dot{W}}{\rho_m^*} \quad \text{(4.4-3)}$$

It is this relationship that is used to change equations (2-33) and 2-38) from differential equations for $\dot{W}$ to differential equations for $\dot{Q}$.

Since the state variable for volumetric flow-based momentum equations is now Q rather than W, the linearizations in the central numerics must be with respect to Q for any flow link with a volumetric flow-based momentum equation.

The details are now presented. In Appendix E (Detailed Numerical Equations and Solution Technique) of Reference 1, all occurrences of ΔW's and subscript W's are replaced by ΔQ's and subscript Q's, respectively, for those flow links that use a volumetric flow-based momentum equation rather than a mass flow-based momentum equation. In other words, the state variable for these links is Q and thus the linearizations are with respect to Q for these links. Two points should be noted about the equations of Appendix E: (1) the quantities Q^M and Q^V refer to heat rates, not volumetric flow rates, but there should be no confusion with the volumetric flowrate Q since the heat rates always appear as superscripted variables; (2) only non-critical flow links (k=1, ..., K) have momentum equations (volumetric or mass based) so the critical flow links (k=K+1, ..., K^*) are in no way impacted. There are two categories of changes in these equations. First, from equation (4.4-3), it is seen that the volumetric flow-based momentum equation is obtained from the mass flow rate-based momentum equation by dividing by ρ_m^*. In Appendix E of Reference 1, the vector and matrix form of the mass-flow-based momentum equation is given by B_W, A_{WW}, A_{WU_M}, A_{WM_M}, A_{WU_V}, and A_{WM_V}. Thus the matrix coefficients B_Q, A_{QQ}, A_{QU_M}, A_{QM_M}, A_{QU_V} and A_{QM_V} are obtained by dividing

B_W, A_{WW}, A_{WU_M}, A_{WM_M}, A_{WU_V}, and A_{WM_V}, respectively, by ρ_m^*. This potentially impacts equations (E-5), (E-53) - (E-56), (E-60) - (E-64), and (E-148) - (E-150). Second, linearizations for flow links with volumetric flow-based momentum equations must be with respect to the state variable Q. This includes A_{QQ}, A_{U_MQ}, A_{M_MQ}, A_{U_VQ}, and A_{M_VQ}. The potentially impacted equations are (E-5), (E-12), (E-19), (E-26), (E-33), (E-35) - (E-38), (E-40), (E-43), (E-46), (E-49), (E-53), (E-54), (E-57), (E-60), (E-65), (E-71), (E-76), (E-82), and (E-148) - (E-151). A_{QQ} involves the linearization of the volumetric flow-based momentum equation with respect to Q and will be covered shortly. First, however, the linearization of the mass and energy equations will be discussed, i.e., the calculation of A_{U_MQ}, A_{M_MQ}, A_{U_VQ}, and A_{M_VQ}.

The derivatives $\frac{\partial}{\partial W_k}(Wh)^M_{i,k}$, $\frac{\partial}{\partial W_k}W^M_{i,k}$, $\frac{\partial}{\partial W_k}(Wh)^V_{i,k}$, and $\frac{\partial}{\partial W_k}W^V_{i,k}$ are replaced by $\frac{\partial}{\partial Q_k}(Wh)^M_{i,k}$, $\frac{\partial}{\partial Q_k}W^M_{i,k}$, $\frac{\partial}{\partial Q_k}(Wh)^V_{i,k}$, and $\frac{\partial}{\partial W_k}Q^V_{i,k}$, respectively, for those non-critical links k (k = 1, ..., K) that have a volumetric flow-based momentum equation. Since $(Wh)^M_{i,k}$, $W^M_{i,k}$, $(Wh)^V_{i,k}$, and $W^V_{i,k}$ are given by equations (2-7) - (2-8) of Reference 1,

$$\frac{\partial}{\partial W_k}(Wh)^M_{i,k} = C^f_{i,k}\cdot\frac{\partial(W_f)_k}{\partial W_k}\cdot(h_{fM})_{i,k} + C^g_{i,k}\cdot\frac{\partial(W_g)_k}{\partial W_k}\cdot(h_{gM})_{i,k}, \tag{4.4-4}$$

$$\frac{\partial}{\partial W_k}W^M_{i,k} = C^f_{i,k}\cdot\frac{\partial(W_f)_k}{\partial W_k} + C^g_{i,k}\cdot\frac{\partial(W_g)_k}{\partial W_k}, \tag{4.4-5}$$

$$\begin{aligned}\frac{\partial}{\partial W_k}(Wh)^V_{i,k} = {} & [1-C^f_{i,k}]\cdot\frac{\partial(W_f)_k}{\partial W_k}\cdot(h_{fV})_{i,k} + \\ & [1-C^g_{i,k}]\cdot\frac{\partial(W_g)_k}{\partial W_k}\cdot(h_{gV})_{i,k},\end{aligned} \tag{4.4-6}$$

and

$$\frac{\partial W^{V}_{i,k}}{\partial W_k} = [1-C^{f}_{i,k}]\ \frac{\partial (W_f)}{\partial W_k} + [1-C^{g}_{i,k}]\cdot\frac{\partial (W_g)_k}{\partial W_k} \qquad (4.4\text{-}7)$$

The analogous derivatives with respect to Q are

$$\frac{\partial}{\partial Q_k}(Wh)^{M}_{i,k} = C^{f}_{i,k}\cdot\frac{\partial (W_f)_k}{\partial Q_k}\cdot(h_{fM})_{i,k} + C^{g}_{i,k}\cdot\frac{\partial (W_g)_k}{\partial Q_k}\cdot(h_{gM})_{i,k}, \qquad (4.4\text{-}8)$$

$$\frac{\partial}{\partial Q_k}W^{M}_{i,k} = C^{f}_{i,k}\cdot\frac{\partial (W_f)_k}{\partial Q_k} + C^{g}_{i,k}\cdot\frac{\partial (W_g)_k}{\partial Q_k}, \qquad (4.4\text{-}9)$$

$$\frac{\partial}{\partial Q_k}(Wh)^{V}_{i,k} = [1-C^{f}_{i,k}]\cdot\frac{\partial (W_f)_k}{\partial Q_k}\cdot(h_{fV})_{i,k} + [1-C^{g}_{i,k}]\cdot\frac{\partial (W_g)_k}{\partial Q_k}\cdot(h_{gV})_{i,k}, \qquad (4.4\text{-}10)$$

and

$$\frac{\partial W^{V}_{i,k}}{\partial Q_k} = [1-C^{f}_{i,k}]\ \frac{\partial (W_f)}{\partial Q_k} + [1-C^{g}_{i,k}]\cdot\frac{\partial (W_g)_k}{\partial Q_k} \qquad (4.4\text{-}11)$$

It can be seen that the only difference between equations (4.4-4) - (4.4-7) and (4.4-8) - (4.4-11) are that $\partial (W_f)_k/\partial W_k$ and $\partial (W_g)_k/\partial W_k$ are replaced by $\partial (W_f)_k/\partial Q_k$ and $\partial (W_g)_k/\partial Q_k$, respectively. These are the derivatives of the phasic mass flow rates with respect to the net flow rate (mass or volumetric). They are calculated as

$$\frac{\partial (W_f)_k}{\partial W_k} = \frac{1}{(\upsilon_f)_k}\cdot\frac{\partial\ (\langle j_f\rangle)_k}{\partial G_k}, \qquad (4.4\text{-}12)$$

$$\frac{\partial (W_g)_k}{\partial W_k} = \frac{1}{(\upsilon_g)_k} \cdot \frac{\partial\ (<j_g>)_k}{\partial G_k}, \tag{4.4-13}$$

$$\frac{\partial (W_f)_k}{\partial Q_k} = \frac{1}{(\upsilon_f)_k} \cdot \frac{\partial\ (<j_f>)_k}{\partial <j>_k}, \tag{4.4-14}$$

and

$$\frac{\partial (W_g)_k}{\partial Q_k} = \frac{1}{(\upsilon_g)_k} \cdot \frac{\partial\ (<j_g>)_k}{\partial <j>_k}, \tag{4.4-15}$$

The derivatives of $<j_f>$ and $<j_g>$ with respect to G are derived from equations (G-24) and (G-25) of Reference 1 and are given in Appendix G as

$$\frac{\partial <j_f>}{\partial G} = \frac{(1-<\alpha>C_o) - \frac{<\alpha>}{\upsilon_g}\left[\frac{\partial}{\partial G} <<V_{gj}>> + <j> \frac{\partial C_o}{\partial G}\right]}{\rho_m^*} \tag{G-38}$$

and

$$\frac{\partial <j_g>}{\partial G} = \frac{<\alpha>C_o - \frac{<\alpha>}{\upsilon_f}\left[\frac{\partial}{\partial G} <<V_{gj}>> + <j> \frac{\partial C_o}{\partial G}\right]}{\rho_m^*} \tag{G-39}$$

The derivatives of $<j_f>$ and $<j_g>$ with respect to j are derived from equation (G-16) and (G-17) of Reference 1 and are

$$\frac{\partial <j_f>}{\partial <j>} = (1 - <\alpha> C_o) - <\alpha> \left[\frac{\partial << V_{gj} >>}{\partial <j>} + <j> \frac{\partial C_o}{\partial <j>}\right] \quad (4.4\text{-}16)$$

and

$$\frac{\partial <j_g>}{\partial j} = <\alpha> C_o + <\alpha> \left[\frac{\partial << V_{gj} >>}{\partial <j>} + <j> \frac{\partial C_o}{\partial <j>}\right]. \quad (4.4\text{-}17)$$

The drift flux routines already return the derivatives of $<<V_{gj}>>$ and C_o with respect to both G and $< j >$ so all the information necessary to calculate $A_{\upsilon,Q}$, $A_{\kappa,Q}$, $A_{u,Q}$, and $A_{\kappa,Q}$ is available.

A_{QQ} involves the linearization of the volumetric flow-based momentum equation with respect to the state variable Q and will be discussed now. Consider now the frictional pressure drop term in equation (2-33) of Reference 1. It is $- C_k | W_k | W_k$ where W is the state variable for mass flow-based momentum equations and where C_k (call it C_k^W for clarity) is the friction coefficient calculated as described in Section 5 of Reference 1. For volumetric flow-based momentum equations one can define the frictional pressure drop term as $- C_k^Q | Q_k | Q_k$ where Q is the state variable and where C_k^Q is related to C_k^W by

$$C_k^Q = \frac{C_k^W}{(\upsilon_k)^2} .$$

υ_k is the specific volume in flow link k. For the new volumetric flow-based momentum equation option in NOTRUMP, there are actually two friction options available. For an input of ITYPEFL = 11, the frictional term is based on the state variable Q_k and on C_k^Q. For an input of ITYPEFL = 21, the form of the frictional term is the original mass flow-based form using W_k and C_k^W. Here it is important to remember that W_k is no longer the state variable so that in the linearization this frictional term must be linearized with respect to Q_k.

In equation (E-60) of Reference 1 for A_{WW} the quantity of $\partial F_k / \partial W_k$ (i.e., $\upsilon = k$) includes the frictional term which is

$$\left(\frac{\partial F_k^W}{\partial W_k}\right)_{friction} = \frac{144\, g_c}{(\Sigma L/A)_k} \cdot 2 \cdot C_k^W \cdot |W_k|$$

For A_{QQ}, the quantity of $\partial F_k / \partial Q_k$ includes the frictional term which for ITYPEFL = 11 is

$$\left(\frac{\partial F_k^Q}{\partial Q_k}\right)_{friction} = \frac{144\ g_c}{(\Sigma L/A)_k} \cdot \frac{1}{\rho_m^*} \cdot 2 \cdot C_k^Q \cdot |Q_k| \qquad (4.4\text{-}20)$$

and for ITYPEFL = 21 is

$$\left(\frac{\partial F_k^W}{\partial Q_k}\right)_{friction} = \frac{144\ g_c}{(\Sigma L/A)_k} \cdot \frac{1}{\rho_m^*} \cdot 2 \cdot C_k^W \cdot |W_k| \cdot \frac{\partial W_k}{\partial Q_k} \qquad (4.4\text{-}21)$$

and where

$$\frac{\partial W_k}{\partial Q_k} = \frac{\partial (W_f)_k}{\partial Q_k} + \frac{\partial (W_g)_k}{\partial Q_k} \qquad (4.4\text{-}22)$$

$\partial (W_f)_k / \partial Q_k$ and $\partial (W_g)_k / \partial Q_k$ are given by equations (4.4-14) and (4.4-15), respectively.

The decision to cast the NOTRUMP momentum equation and the drift flux equations in terms of net volumetric flow rate rather than mass flow rate is based on the following. Most state-of-the-art codes such as TRAC and RELAP5 use velocity-based momentum equations. It is generally accepted that drift flux is more easily applied and more successful in a volumetric-flow context because drift flux is basically a volumetric-flow or velocity concept.

Note: The final NOTRUMP V&V report will contain a list of variable nomenclature. The following nomenclature will be included in the list.

A	=	flow area (ft^2)
C_o	=	drift flux distribution parameter
G	=	total mass flux (lbm / sec / ft^2)
h	=	specific enthalpy (Btu / lbm)
j	=	volumetric flux (ft^3 / sec / ft^2)
Q	=	volumetric flow rate (ft^3 / sec)
$\dot{Q}$	=	time rate of change of Q (ft^3 / sec^2)
V_{gj}	=	drift velocity of vapor relative to the total volumetric flux (ft / sec)
W	=	net mass flow rate (lbm / sec)
$\dot{W}$	=	time rate of change of W (lbm / sec^2)
X	=	quality (-)
ρ	=	density (lbm / ft^3)
υ	=	specific volume (ft^3 / lbm)
α	=	void fraction

Subscripts:

f	=	liquid phase
g	=	vapor (gas) phase

Reference

440.469-1 P. E. Meyer, et. al., "NOTRUMP - A Nodal Transient Small Break and General Network Code," WCAP-11079-P-A (Proprietary), WCAP-10080-A (Non-proprietary), August 1985.

SSAR Revision: NONE

Question 440.472

Re: NOTRUMP PVR FOR OSU TESTS, LTCT-GSR-001, JULY 1995

In Section 4.7, liquid reflux flow links were added to prevent the nonphysical depressurization of nodes with no mixture regions when subcooled liquid enters. Adding subcooled liquid from the hot legs to a lower core node, for example, could result in artificially cooling the fuel. Please demonstrate that artificially adding the subcooled liquid to the mixture region below the upper steam regions in the core does not artificially cool the fuel. Also, how does this methodology affect level swell, bubble rise, and steam production in the mixture region to which the subcooled liquid is added? Please explain in detail.

Response:

As stated in Section 4.7 of LTCT-GSR-001 and PXS-GSR-002, the new internally calculated liquid reflux flow links are a generalization of the NOTRUMP model for hot leg to reactor vessel reflux which is described in Sections 3-1-10 through 3-1-12 of Reference 440.472-1. This model which was approved in the NOTRUMP SER is still used for the reactor vessel. For AP600 applications, the new generalized model is used for the steam generators primary sides, for the CMT's, and for the multi-node downcomer of the SPES-2 facility. Even though the model for hot leg to reactor vessel reflux has not been changed, its impact will be discussed.

The RAI asks for an explanation of why adding the subcooled liquid to the mixture region below the upper steam regions in the core does not artificially cool the fuel. This request assumes that the core is uncovered since it refers to "steam regions in the core." The core does not actually uncover for AP600 during small break LOCAs. If the core were to uncover however, then the steam above the core mixture level would be superheated and at least some of the core region below the mixture level would likely contain a two-phase saturated mixture. In this situation, most of the liquid entering at the top of active core region would be expected to fall to the mixture level while slightly de-superheating the steam above the mixture level and reducing the quality of the two-phase mixture just below the mixture level. The NOTRUMP model for hot leg to reactor vessel reflux would, in this situation, put the reflux liquid into the mixture region just below the mixture level (i.e., into the mixture region of the stacked mode containing the single stack mixture elevation). This mixture region would most likely be two-phase. In this case, the reflux liquid, whether saturated or subcooled, would reduce the quality of the mixture region but not alter its temperature. In the unlikely case that the mixture region were subcooled, then the reflux liquid would alter the temperature of the region in a manner depending on the temperature of the reflux liquid to the temperature of the subcooled region. (The temperature could increase or decrease.) For this unlikely case, however, the fuel would be well-cooled anyway, so that this altering of the mixture region temperature would have little impact. The NOTRUMP model does not account for the slight de-superheating of the superheated vapor above the core mixture level as the reflux is directed to the mixture level. This is conservative during core uncovery because: (1) by keeping the superheated vapor hotter, it keeps the exposed fuel (i.e., the fuel above the mixture level) hotter; and (2) by not de-superheating (or even saturating and condensing) the vapor, it keeps the level depressed.

If this is contrasted to the nonconservative and physically less realistic case of no reflux links, the reflux liquid would desuperheat and possibly condense all the vapor as the reflux liquid instantly comes to thermal equilibrium with the steam above the core. This would not only unrealistically depressurize the regions above the core mixture level but also nonconservatively cool any exposed fuel and cause the mixture level to rise.

In the NOTRUMP SER, the NRC found the NOTRUMP core model, of which the hot leg to reactor vessel reflux model is an integral part, to be acceptable. Based on this assessment, it was felt to be unnecessary to change the model for hot leg to reactor vessel reflux for AP600 calculations. It was decided, however, to generalize the model for use in other components of the AP600 (e.g., steam gene-ator tubes, CMT's, and multi-node downcomers). It is the generalization that is described in Section 4.7 of LTCT-GSR-001 and PXS-GSR-002.

Reference

440.472-1 N. Lee, et. al., "Westinghouse Small Break ECCS Evaluation Model Using the NOTRUMP Code," WCAP-10054-P-A (Proprietary), WCAP-10081-A (Nonproprietary), August 1985

SSAR Revision: NONE

Question 440.484

Re: NOTRUMP PVR FOR OSU TESTS, LTCT-GSR-001, JULY 1995
Please provide a clad temperature calculation to show the effect of the changes to the transition boiling correlation calculation on peak clad temperature for a heatup transient that experiences transition boiling heat transfer.

Response:

Section 4.19 of LTCT-GSR-001 and PXS-GSR-002 describes the changes implemented to the numerical solution technique employed in NOTRUMP heat links when the Westinghouse Transition Boiling Correlation is used. The details of the calculations for NOTRUMP heat links are given in Section 6 of Reference 440.484-1. It must be pointed out that NOTRUMP heat links are not used to model core heat transfer. The core fuel rod model and its associated heat transfer correlations, described in Appendix T of Reference 440.484-1, are used to model core heat transfer. No changes have been made to this model for AP600 applications. As such, the request for a clad temperature calculation to show the effect of the changes described in Section 4.19 on peak clad temperature is not applicable. Also, since the core does not uncover, it does not experience transition boiling.

Reference

440.484-1 P. E. Meyer, et. al., "NOTRUMP - A Nodal Transient Small Break and General Network Code," WCAP-10079-P-A (Proprietary), WCAP-10080-A (Nonproprietary), August 1985

SSAR Revision: NONE

Question 440.505

Re: NOTRUMP PVR FOR OSU TESTS, LTCT-GSR-001, JULY 1995
Please explain the source of the oscillations in break flow from about 150 to 240 seconds and 340 to 430 seconds in Fig. 5.4-24. Please explain why the NOTRUMP code does not simulate the data nor trends and underpredicts the break flow from 120 seconds until the end of the transient at 500 seconds.

Response:

In the NOTRUMP simulations, the oscillations seen between 150 and 210 seconds are due to water from Accumulator 1 injection periodically recovering the break link, leading to alternating vapor and liquid flow out of the break. Similarly, the oscillations between 340 and 430 seconds are due to IRWST injection into the broken DVI line periodically recovering the break. This effect is a direct result of the discretization implicit in NOTRUMP. Such effects are typical of what has been seen qualitatively in other computer simulations when modeling the break and the cold leg refilling behavior. As was stated in the OSU preliminary validation report, final test data was not available when these comparisons were made. When one calculates the break flow rate in the test by adding the CMT flow (determined from the rate of change of the mass in the C..IT) to the accumulator flow, and compares it to the same quantities in the NOTRUMP calculation as shown in Figures 440.505-1, the agreement is much better. Note that this comparison has been adjusted to eliminate the flow component from the IRWST injection line in the NOTRUMP simulation to maintain consistency with the quantity plotted in the new test data curve. At approximately 130 seconds, both the test data and the NOTRUMP simulation predict a short period of predominantly vapor flow until Accumulator 1 resumes flow. During the following accumulator injection period, the flows again are similar, except for the oscillations explained above.

SSAR Revision: NONE

(a,b)

Figure 440.505-1 CMT and Accumulator Mass Flow Rate for OSU Test SB12

Question 480.214

Re: Questions on OSU/APEX Sump Behavior:
Review of the tests in the OSU/APEX facility has resulted in uncertainty about (1) the modeling of the containment sump in the facility, and (2) how the "primary" sump communicates with both the "secondary" sump and the reactor cooling system.

In the Test Specification for APEX, Section 6.0, p. 16, it is stated, "A vessel shall be provided to simulate the flooded volumes in the lower containment. This vessel shall be sized to contain all water from the reactor coolant system (RCS), ACCS, CMTs, and in-containment refueling water storage tank (IRWST)." There is no differentiation in this statement between the primary and secondary sumps, nor how the volume of the two sump tanks is apportioned to represent the AP600 sump. However in the APEX scaling report, Section 7.3, p. 7-11, it is stated, "The containment sump will accommodate all of the IRWST, CMT, and accumulator liquid volumes." (Note that the RCS does not appear.) The APEX scaling report goes on to relate the primary sump tank and the secondary sump tank to lower containment volumes available for recirculation to the RCS (referred to as the sump) and those that are not available for recirculation (referred to as "normally non-flooded"), respectively. The "curb" or "spillover" elevation is denoted as that point at which fluid filling the non-flooded volumes would spill over into the sump. Part of the question about sump tank volumes relates to the total liquid volumes and accommodation thereof in the sump. It is also stated in the scaling report that the relative elevations, volumes, and the "spillover" elevation of the primary and secondary sumps are properly scaled in APEX.

a. The total volume of the containment sump, up to the "curb" elevation, is given in the APEX Scaling Report as 58,263 ft3. However, the total liquid volume in the CMTs, accumulators, and IRWST is: 2000 ft3 per CMT; 1700 ft3 per accumulator; and, as given in Section 6.5.3.1, p. 6-93 of the Scaling Report, the IRWST volume is 70,798 ft3. The total of these volumes is thus 78,198 ft3. Reconcile the mismatch between the total volume and the sump volume, in light of the quoted statement on p. 7-11 regarding the capability of the sump to accommodate these volumes. Note: Also address the statement in the APEX Test Specification regarding accommodation of these volumes plus that of the RCS, given that the RCS volume adds another 7280 ft3 to the total volume. (Volume of RCS taken from AP600 standard safety analysis report (SSAR), Table 5.1-2.)

b. How much liquid volume must exist in the sump to flood to an elevation adequate to permit recirculation from the sump to the RCS?

c. The "normally non-flooded" containment volume is given on p. 7-11 of the scaling report as 35,403 ft3. Demonstrate that, if a break were to occur such that these compartments were the first to flood, enough water would flow over the "curb" into the sump to flood the sump to a level permitting recirculatory cooling.

Response:

a. The primary and secondary sumps at the OSU test facility were scaled to represent the normally flooded and unflooded containment compartments respectively. The total "sump" volume, both primary and secondary, is equivalent to the sum of all the compartments and is sufficient to accomodate the volumes of the IRWST, CMTs, accumulators, and RCS.

b. The plant design has the direct vessel injection centerline at the 99' 7" elevation. In order to permit recirculation, the sump (containment compartments) must flood to this elevation, plus the RCS pressure. The design floodup elevation (including flooding of one of the normally non-flooded compartments) is 107 feet.

c. For the AP600 design, as presented in the OSU scaling report, should a loss of coolant occur in one of the "normally non-flooded" compartments of containment, this compartment would be the first to fill. The water would then overflow into the normally flooded areas. Using the numbers provided in Table 8-9 of the scaling report, the normally non-flooded volume (two non-flooded compartments) was 35,403 ft^3 and the sump volume below the DVI was 37,063 ft^3. Using 85,478 ft^3 as the volume for the IRWST, CMTs, accumulators, and RCS, and subtracting the non-flooded containment volume and the sump volume below the DVI, the volume available for flooding above the DVI elevation was 13012 ft^3. Table 8-9 provides a cross sectional area for the sump above the DVI elevation as 2793 ft^2. This results in 4.7 feet of water elevation above the DVI line.

Note however that the OSU secondary sump is representative of several normally non-flooded containment compartments. If such a break were to occur, only one of the normally non-flooded compartments would fill with water. Also, these compartments now have drain connections to the normally flooded area (OSU primary sump). The normally non-flooded compartment would rise concurrently with the normally flooded area.

SSAR Revision: NONE

Question 480.215

Re: Questions on OSU/APEX Sump Behavior:
As the IRWST drains and the sump fills, recirculatory cooling will eventually switch over from the IRWST to the sump. If there is no overlap between the water level in the sump and that in the IRWST when IRWST injection ceases, there may be a delay in sump injection, or a reduction in recirculation flow into the RCS. Show that for the scenario postulated in 1.c. above, either that (a) there is an adequate overlap between sump and IRWST levels to prevent cessation or reduction in RCS flow, or (b) that any such effects would be of sufficiently brief duration so as not to result in unacceptable core cooling conditions.

Response:

The OSU secondary sump is representative of several normally non-flooded containment compartments. These compartments have drain connections to the normally flooded area (OSU primary sump). If a break were to occur in one of these compartments, this compartment, which is a portion of the non-flooded area, would fill with water concurrently with the normally flooded area. The floodup level with one normally non-flooded compartment and the normally flooded area together is 107 feet. The bottom of the IRWST is 103 ft., therefore, sufficient overlap exists to prevent cessation of RCS flow.

SSAR Revision: NONE

Question 480.244

Re: Test OSU-F-01:
The data on ADS lines is not usable, because the lines did not stay full as planned. Westinghouse should explain how these lines will be characterized for use of the information in analysis codes.

Response:

During the course of testing, the field engineer opened RCS-620, located at the top of the separator, and came to the conclusion that, because there was no water issuing from the vent line, the lines leading to the separtor were not full. The Quick Look Report (LTCT-T2R-002) reported this conclusion. However, as the test data was analyzed more fully, there was evidence that the ADS separator inlet lines were completely filled with water and that pressure in the separator forced the water through the liquid drain line. A complete discussion of the test, including estimated line resistances and pressure drops is presented in Section 4.2.9.3 of Reference 480.244-1.

Reference

480.244-1 WCAP-14252, "AP600 Low Pressure Integral System Test at Oregon State University: Final Data Report," Proprietary [LTCT-T2R-100], May 1995.

SSAR Revision: NONE

Question 480.245

Re: Test OSU-HS-01:
The staff notes that the data for ambient heat losses at 100 F is unusable. Westinghouse indicates that the test is acceptable even though this part of the test was not completed. Westinghouse should justify the acceptability of the test in light of its failure to achieve one of its objectives.

Response:

The purpose of the HS-01 hot functional test was to obtain data under a variety of conditions to determine OSU facility characteristics. It was virtually impossible to maintain stable conditions at the low steam and feedwater rates necessary to maintain 100°F. However, usable data was obtained for the facility at 200°F, 300°F, and 400°F. This data provided an adequate characterization of the facility heat loss, therefore the test was acceptable.

SSAR Revision: NONE

Question 480.252

Re: Test OSU SB1:
There appear to be some instruments that are not properly zeroed. For instance, see Plots 26, 27, and 28, for the accumulator level and pressure. These errors should be accounted for in Westinghouse's analysis.

Response:

As noted in the Quick Look Report for SB1, the Bourdon pressure tube indicator PI-401 (PI-402) was tubed to the lower portion of the reference leg for differential pressure transmitter LDP-401 (LDP-402). As pressure in the accumulator was increased, the air inside the Bourdon tube was compressed, thereby lowering the reference leg liquid level. This resulted in a false indication of measured level which was reported in Reference 480.252-1 and corrected, when used, in the analyses performed in Reference 480.252-2.

Reference

480.252-1 WCAP-14252, "AP600 Low Pressure Integral System Test at Oregon State University: Final Data Report," Proprietary [LTCT-T2R-100], May 1995.

480.252-2 WCAP-14292, Revision 1, "AP600 Low-Pressure Integral Systems Test at Oregon State University Test Analysis Report," Proprietary [LTCT-T2R-600], September 1995.

SSAR Revision: NONE

Question 480.253

Re: Test OSU SB1:
The description of events in the beginning of the report (p. 6-2) leaves out a great deal of information. For example, the timing for various features described for instruments LDP-115 and LDP-127 appears to be different from that seen on the plots; in addition, the description of the behavior of LDP-140 leaves out a number of dynamic features (e.g., the sharp spikes at about 4000 and 5000 seconds that have been shown by the staff to be associated with CMT refill). The staff expects that a much more thorough analysis of the dynamic systems interactions noted in this and other similar tests will be undertaken in future reports on the APEX testing.

Response:

The Quick Look Report was used as a mechanism to provide data to reviewers in a timely manner. Therefore, an evaluation of all test phenomena was not provided. The Quick Look Reports have been superseded by References 480.253-1 and 480.253-2. For discussions of SB01, a 2-inch break in the bottom of the cold leg, see section 5.1.1 of Reference 480.253-1 and section 5.1 of Reference 480.253-2.

Reference

480.253-1 WCAP-14252, "AP600 Low Pressure Integral System Test at Oregon State University: Final Data Report," Proprietary [LTCT-T2R-100], May 1995.

480.253-2 WCAP-14292, Revision 1, "AP600 Low-Pressure Integral Systems Test at Oregon State University Test Analysis Report," Proprietary [LTCT-T2R-600], September 1995,

SSAR Revision: NONE

Question 480.254

Re: Test OSU SB1:
Negative gage pressures are shown for several instruments, including pressurizer pressure (Plot 18) and ADS 1-3 separator pressure (Plot 53). These need to be explained.

Response:

As described in section 5.1.1 of Reference 480.254, the negative pressures seen on the pressurizer and ADS 1-3 separator pressure were due to the lack of a vacuum breaker on the sparger line inside the IRWST. At approximately 2000 seconds, the pressurizer surge line began to refill. At approximately 3200 seconds, the pressurizer began to reflood. Also at this time, the sparger nozzles were still submerged. As the piping and components cooled between the pressurizer and the sparger, the steam condensed inside and the pressure fell, resulting in a slight vacuum in this line. A vacuum breaker was installed following this test.

Reference

480.254-1 WCAP-14252, "AP600 Low Pressure Integral System Test at Oregon State University: Final Data Report," Proprietary [LTCT-T2R-100], May 1995.

SSAR Revision: NONE

Question 480.255

Re: Test OSU SB1:
What effect, if any, results from the top of the CMT being heated to approximately 150°F prior to the beginning of the test?

Response:

As indicated in section 5.1.1 of Reference 480.255-1, CMT-2 temperature indicated by TF-532 was 154.7°F. However, further data provided in Reference 480.255-1 indicates that less than 15 percent of the CMT volume was at a temperaure greater than 80°F. Although this elevated temperature will affect CMT performance (slightly less mass in the CMT resulting in a slower recirculation rate), analysis of the test using the elevated initial temperature is still possible.

Reference

480.255-1 WCAP-14252, "AP600 Low Pressure Integral System Test at Oregon State University: Final Data Report," Proprietary [LTCT-T2R-100], May 1995.

SSAR Revision: NONE

Question 480.256

Re: Test OSU SB3:

The staff notes that the CMT temperature again was significantly elevated near the top. This is not specifically attributed to the PBL warmup prior to the test, but it is assumed that this is the explanation. It would be valuable, however, to include such notes either in initial conditions list or, even better, in the Test Procedure section, rather than simply stating that the test was performed according to an established procedure. This type of information helps the staff differentiate true anomalous indications from those that are easily explainable by virtue of facility operation procedures.

Response:

As noted, the elevated CMT temperature was due to pressure balance line warmup prior to the test. Section 2.7 of the Reference 480.256-1 provides a discussion of the pre-test operations that were performed prior to each of the matrix tests. In addition, a discussion of the system configuration and initial conditions is provided for each matrix test discussed in Section 5 of Reference 480.256-1.

Reference

480.256-1 WCAP-14252, "AP600 Low Pressure Integral System Test at Oregon State University: Final Data Report," Proprietary [LTCT-T2R-100], May 1995.

SSAR Revision: NONE

Question 480.257

Re: Test OSU SB3:
The erratic response on the PRHR HX outlet flow (Plot 44) is somewhat puzzling to the staff, since it would be expected that this would be in single phase flow, unless these is ingress of non-condensible gas. Please explain.

Response:

As is the case with many of the tests, during accumulator injection the PRHR flow decreased to near zero and the PRHR level decreased. The PRHR HX inlet fluid temperature became subcooled and began to decrease. This was an indication that there was no flow through the PRHR heat exchanger. The erratic response of the PRHR HX outlet flow may have been due to either the outlet line which was not completely full or to oscillations of the liquid in the loop seal between the bottom of the heat exchanger and the steam generator.

SSAR Revision: NONE

Question 480.259

Re: Test OSU SB3:
Explain why power is not listed as a specified initial condition. Also, at the end of the test, the power meters go negative. Is this an expected response, or does it raise questions about the accuracy of the power measurements during the test? Finally, the staff notes that the power is increased in a step fashion just before the test begins. Presumably this is a planned event; however, it is not described in the Test Procedure section nor in the list of initial conditions. This type of action needs to be flagged and explained.

Response:

The AP600 Low Pressure Integral Test at Oregon State University Final Data Report, May 1995, section 2.6.12 describes the control algorithm used to simulate the decay power expected in the AP600 plant scaled to the OSU Test Facility. For all matrix tests except SB21, the control algorithm was:

For $0 < \text{time} \leq 140$ seconds; power (KW-101 or KW-102) = 300 kW
For time > 140 seconds; power (KW-101 or KW-102) = $300/[1 + B(t-140)]^C$

The Matrix Test SB21 decay power algorithm was:

For $0 < \text{time} \leq 140$ seconds; power (KW-101 or KW-102) = 300 kW
For time > 140 seconds; power (KW-101 or KW-102) = $300/[1 + B(t-140)]^C$

where: B = 0.01021 and C = 0.2848

Prior to time zero, the test facility was controlled to maintain the hot leg temperature specified and not to a specific power level. At time zero, the power would change to 300 kW. Power is therefore not specified as an initial condition.

At the end of the test, the indicated power is negative. This is an expected response on the DAS to opening of the reactor breakers. It does not raise questions about the accuracy of the power measurements during the test.

SSAR Revision: NONE

Question 480.260

Re: Test OSU SB3:
The BAMS discharge line thermocouples (Plots 75, 76) show considerably different behavior. TF-916 shows that the discharge is largely saturated during the long term portion of the test. However, TF-917 (signal conditioned output) shows significant subcooling in the exhaust flow. Explain this apparent discrepancy.

Response:

Hot leg temperatures (plots 13, 14, 15, 16) indicate that the hot legs are subcooled from about 3800 seconds to about 8000 seconds. This would indicate that no steam is leaving the vessel and exiting the BAMS during this time. Thermocouple TF-917 was on the line used for steam flow during this test. Thermocouple TF-916 was on a closed line. When steam flow dropped, TF-917 experienced a gradual cooldown. When steam flow began again at about 8000 seconds, the cooldown ended and the temperature again began to rise to saturation. Also, it should be noted that the two thermocouples of in two different heat traced zones which are operated by independent controllers. The differences in temperatures are due to a combination of the heat tracing, the open vs. closed pipe, and the steam flow.

SSAR Revision: NONE

Question 480.263

Re: Test OSU SB9:
There appears to be a significant number of failed and/or erratic instrumentation in this test, and there is an admission that not all instruments met specified acceptance criteria. There is no "critical instrument" list provided, no specific indication as to whether any of the failed instruments would have been considered "critical," and no indication how missing critical instrumentation was compensated for. Since this is a "blind" test, with no data presented in the QLR for review, there is no way to confirm at this time that Westinghouse's judgement regarding the acceptability of this test is reasonable. The staff will review the data from this test when it is provided.

Response:

The Quick Look Report was used as a mechanism to provide data to reviewers in a timely manner. Therefore, an evaluation of all phenomena was not provided. The Quick Look Reports have been superseded by References 480.263-1 and 480.263-2. The performance of any failed instruments on the critical instrument list is assessed for each test in Reference 480.263-1 as to the test acceptability. For discussions of SB09, a 2-inch break in the bottom of the cold leg, see section 5.3.2 of the Reference 480.263-1 and section 5.4 of Reference 480.263-2.

Reference

480.263-1 WCAP-14252, "AP600 Low Pressure Integral System Test at Oregon State University: Final Data Report," Proprietary [LTCT-T2R-100], May 1995.

480.263-2 WCAP-14292, Revision 1, "AP600 Low-Pressure Integral Systems Test at Oregon State University Test Analysis Report," Proprietary [LTCT-T2R-600], September 1995,

SSAR Revision: NONE

Question 480.264

Re: Test OSU SB12:
Thermocouples in CL1 and CL3 (TF-107 and TF-103, Plots 5 and 9, respectively) show step decreases in temperature at about 6600 seconds. These do not appear to be associated with any liquid level changes in the cold legs (see Plots 103, 104). Explain this behavior.

Response:

As indicated in Table 5.4.1-2, Matrix Test SB12 Inoperable Instruments/Invalid Data Channels, of the OSU TDR, the data from LDP-201 through LDP-206 was invalid due to the effect of the vertical portion of the sense line which was attach to the top of the pipe. However, if the downcomer level compared with the temperature drop, it can be seen that the temperature decrease is associated with downcomer level approaching the cold leg elevation.

SSAR Revision: NONE

Question 480.265

Re: Test OSU SB12:
Why do CL2 and CL4 (Plots 105, 106) partially refill between about 2500 and 5000 seconds? They then appear to empty, even though the vessel and downcomer levels continue to rise.

Response:

As indicated in Table 5.4.1-2, Matrix Test SB12 Inoperable Instruments/Invalid Data Channels, of Reference 480.265-1, the data from LDP-201 through LDP-206 was invalid due to the effect of the vertical portion of the sense line which was attach to the top of the pipe. Once the pipe began to drain, this portion of the sense line drained resulting in invalid level indications.

Reference

480.265-1 WCAP-14252, "AP600 Low Pressure Integral System Test at Oregon State University: Final Data Report," Proprietary [LTCT-T2R-100], May 1995.

SSAR Revision: NONE

Question 480.266

Re: Test OSU SB12:
Why to the hot legs (Plots 101, 102) appear to refill to a level above their initial values?

Response:

As indicated in Table 5.4.1-2, Matrix Test SB12 Inoperable Instruments/Invalid Data Channels, of the OSU TDR, the data from LDP-201 through LDP-206 was invalid due to the effect of the vertical portion of the sense line which was attach to the top of the pipe. Once the pipe began to drain, this portion of the sense line drained resulting in invalid level indications.

SSAR Revision: NONE

Question 480.271

Re: Test OSU SB14:
Why are the initial levels different on Plot 110 (comparison of LDP-115 from tests SB14 and HS-03)?

Response:

As stated in section 2.4.3.1 of Reference 480.271-1, LDPs measure fluid level between the upper reference leg tap and the lower variable leg tap of a component. Flow in a component creates a dynamic differential pressure due to the pressure loss beween the component LDP taps as fluid flows through the component. When this dynamic component of differential pressure is superimposed on the static differential pressure, the resulting transmitter signal produce invalid data. Therefore, the LDPs in the vessel during flowing conditions should not be used directly.

Reference

480.271-1 WCAP-14252, "AP600 Low Pressure Integral System Test at Oregon State University: Final Data Report," Proprietary [LTCT-T2R-100], May 1995.

SSAR Revision: NONE